Voyager Interstellar

A Description of the Voyager Plasma Science Instrument and Data

(Equations are created using *MathType*: *https://www.wiris.com/en/mathtype/*)

Table of Contents

1 Overview 4
1.1 Dates of Magnetospheric Encounters 5
1.2 Crossing of the Termination Shock and the Heliopause 5
1.3 Voyager 1 Hardware Failure Dates 5
1.4 Data, Documentation, and Software: *Voyager_PLS_v_02/* 6
1.4.1 Voyager_PLS_v_02/documentation_v_02/ 6
1.4.1.1 *Voyager_PLS_v_02/documentation_v_02/general* 6
1.4.1.2 *Voyager_PLS_v_02/documentation_v_02/encounter_papers* 8
1.4.1.3 *Voyager_PLS_v_02/documentation_v_02/publications* 8
1.4.1.4 *Voyager_PLS_v_02/documentation_v_02/voyager_memos* 8
1.4.2 Voyager_PLS_v_02/McNutt 9
1.4.3 Voyager_PLS_v_02/software_v_01/ 10
1.4.4 Voyager_PLS_v_02/v1/ 10
1.4.5 Voyager_PLS_v_02/v2/ 11
1.4.6 Flash Drive for Transferring Data and Software (for MIT users only). ... 11
1.5 An Informal History of the PLS Processing at MIT and GSFC 12
1.5.1 Summary Tape Processing at *GSFC* 12
1.5.2 Production of Mission (*vgr*) files at *MIT* 13
1.5.2.1 Millisecond Timing Issues on Mission files 13
1.5.2.2 The Full Answer Array 14
1.5.2.3 Limitations of the Mission files 14
1.5.2.4 *SPC* and *V1/2all files* 15
1.5.3 *SPL* files for the encounters 15
1.5.4 The Full Response Function and *MJSANL* 16
2 Spacecraft and *PLS* Instrument 16
2.1 Configuration 16
2.2 Spacecraft coordinates and cup normals 17
2.3 The Canopus Sensor 19
3 Instrument 19
3.1 The Experimental Concept 19
3.1.1 Voltage Levels 19
3.1.1.1 *L-Mode* 20
3.1.1.2 *M-Mode* 21
3.1.2 Reduced Distribution Function and Measured Currents 24
3.1.3 Moments Calculation 25
3.1.4 Relationship between Pressure, Temperature, and Thermal Speed 26
3.1.5 Theoretical Examples of the Voyager Measurement Scheme 27

3.2 Measured Voyager Ion Spectra 28
3.2.1 Solar Wind M Modes 28
3.2.2 Heliosheath L Modes 29
3.2.3 Fitting a Bi-Maxwellian to Voyager Spectra Assuming Unit Response 29
3.2.4 Non-Linear Least Squares Fitting 30
3.3 The Measurement Sequence and *M* Start Words 32
3.4 The Status Word 33
3.4.1 Bits 1 and 2 of status word code L, E1, E2, M 33
3.4.2 Bits 3 and 4 of status word code IGAIN and ICAP 34
3.4.3 Values of bits 1-4 of status word in hexadecimal 34
3.4.4 Bits 5 through 8 of status word code calibration modes 35
3.4.5 Code for Status Word Decoding 35
3.5 DN (digital numbers) and EU (engineering units) 36
3.5.1 Determining the Threshold 36
3.5.2 Formula for Conversion DN to EU 37
3.6 Time Interval between Measurements 37
3.6.1 Typical Intervals 37
3.6.2 12 Second Measurements 37
4 Code Snippets Data Analysis 38
4.1 Voyager constants: *plsbeg.f* 38
4.2 Converting Digital Number (DN) Values to Currents: kntcur.f 38
4.3 Generating Voltages and Speeds for Energy Channels: step.f 39
4.4 Calculating Plasma Moments: *moment.f* 39
4.5 Moment Analysis of Proton Data: *pranal.f* 41
4.6 Manipulating bits in the status word: *l1x* 42
5 Trajectory and Pointing 42
5.1 Coordinate Systems 42
5.1.1 Earth Equatorial to Ecliptic ECL50 42
5.1.2 ECL50 43
5.1.3 RTN Heliographic 43
5.1.4 IHC Interstellar Heliospheric Coordinates 45
5.1.5 Going from Measured Cup Speeds to Velocity in *RTN* or *IHC* 46
5.2 Lock stars 46
5.3 Generating Pointing Given the Lock star and $Z_{s/c}$ 47
5.4 Short *SEDR* File Format for Cruise 47
5.5 Short *SEDR* File Format for Encounters 48
5.5.1 Jupiter 48
5.5.2 Saturn 50
5.5.3 Uranus 50
5.5.4 Neptune 51
6 Code Snippets Trajectory/Pointing Data 52
6.1 Lock Stars: *refer.f* 52
6.2 Transforming from *ECL50* to *RTN* (solar heliographic): *helio.f* 54
7 *PLS* Cruise and Encounter Data and Calibrations 55
7.1 Calibration files 55
7.1.1 Modulator Voltage Calibration 56

7.1.2 Current Calibrations 58
7.2 Daily and hourly averages, and fine resolution data 59
7.3 Mission Files (*vgr* files) 59
7.4 Spectral Files and Color Spectrograms (*spc* files and plots) 61
7.5 Encounter Files (*spl* files) 62
7.6 Summary Files (*summary*) 63
7.7 Experimental Data Record Files (*edr*) 64
8 Analysis of Data in the Interstellar Medium 64
8.1 Description 64
8.2 Roll Times 65
9 Data from the Last EDR 70
10 List of Voyager Memos 72
11 Differences between VOY_PLS_V01 and VOY_PLS_V02 75

1 Overview

See Section 11 for a description of how *VOY_PLS_V02* (described here in this document, *VoyagerInterstellar_v_07*) differs from *VOY_PLS_V01* (described in an earlier version of this document, *VoyagerInterstellar_v_06*) differ.

VOY_PLS_V02 is a flash drive containing the following:

1. A folder *Voyager_PLS_v_02* which contains all the *PLS* data from launch through failure (Voyager 1) or turn off (Voyager 2), plus various software routines used to analyze this data.
2. A folder *tar_files* which contains 25 *tar.gz* files with the PLS data for the entire mission in *tar* form.
3. A text file *VOY_PLS_V02_readme.txt*, which explains the contents of the flash drive and how to deploy the contents.
4. An executable bash script *script_for_PLS_deploy* to unzip and untar the tar files after being dragged onto the desired directory on your laptop (drag the executable and the tar_files folder into the desired directory. This will create a folder on your laptop *Voyager_PLS_v_02* in the desired directory identical to the one on this flash drive.
5. An executable bash script *script_for_PLS_deploy_flashdrive* to unzip and untar the *tar_files* tar files after being dragged to the appropriate directory on your laptop, back to a flash drive. This will create a folder on your flash drive *Voyager_PLS_v_02* identical to the one on this flash drive.

Important note: on the original *VOY_PLS_V01* flash drive I had not properly untarred the spectrogram plots from Voyager 1 onto the flash drive itself (they were properly in the tar files on *VOY_PLS_V01* and if you untarred them using *script_for_PLS_deploy* you got everything correctly installed on the laptop you were transferring them to)

But the *script_for_PLS_deploy_flashdrive* on *VOY_PLS_V01* had an error in it such that the Voyager 1 histogram plots were not included the flash drive itself in *E:\Voyager_PLS_v_01\v1\spc*). If you have one of these flash drives *VOY_PLS_V01* **please rename and repurpose it**, so that copies of this are not floating around. The *script_for_PLS_deploy_flashdrive* on *VOY_PLS_V02* has been corrected.

The contents of *VOY_PLS_V02* at MIT are in */nfs/faraday/data/jwb/Voyager_PLS_v_02*.

The complicated history of the PLS processing at MIT and GSFC over the 47 years of the mission, is sketched in Section 1.5 below. I have put together a set of data, software, and documentation for the Voyager PLS experiment, in the directory *Voyager_PLS_v_02*. The main documentation consists of three documents:

Voyager Interstellar: A Description of the Voyager Plasma Science Instrument and Data

MJSANL: The Positive-Ion Least-Squares Fitting Routine for the Voyager PLS Instrument

The Voyager PLS Utility Software

The most recent versions of these documents are *VoyagerInterstellar _v_07*, *MJSANL_v_02,* and *VoyagerPLSUtilitySoftware_v_01*. See Section 1.4.1.1 below.

The PLS experiment was turned off on September 27, 2024. See Section 9 for the last *LEME* sequence from the instrument.

1.1 Dates of Magnetospheric Encounters

The launch dates of the Voyager I and II spacecraft were September 5 and August 20, 1977, respectively. The Voyager 1 instrument failed for the final time after the Saturn encounter, near 1980 328 1024:14. Table 1 gives the times of the various planetary encounters. We discuss here the PLS experiment's location on the spacecraft and its measurement capabilities, including data and trajectory information for the mission.

Table 1-1: Voyager Flybys of Jupiter, Saturn, Uranus and Neptune – BS-BS

	First Bow Shock	Last Bow Shock	Duration (hrs)	M-Modes	L-Modes	E-Modes
Jupiter V1	1979 059 1434	1979 081 1302	529	3.2 min	96 sec	96 sec
Jupiter V2	1979 183 1619	1979 215 1703	1297	3.2 min	96 sec	96 sec
Saturn V1	1980 316 2326	1980 321 0619	103	3.2 min	96 sec	96 sec
Saturn V2	1981 236 1338	1981 243 0108	155	3.2 min	96 sec	96 sec
Uranus V2	1986 024 0715	1986 029 0600	118	12 mins	48 sec	48 sec
Neptune V2	1989 236 1438	1989 240 0600	88	12 mins	48 sec	48 sec

1.2 Crossing of the Termination Shock and the Heliopause

Voyager 2 crossed the termination shock of the solar wind at least five times on DOY 242 to 244, 2007. It crossed into the interstellar medium on DOY 309, November 5, 2018. The science papers for each encounter and for the two boundary transitions can be found in

Voyager_PLS_v_02/documentation_v_02/encounter_papers.

See Section 1.4.1.3 below.

1.3 Voyager 1 Hardware Failure Dates

The Plasma Science experiment on Voyager 1 suffered two major failures after launch in September 1977. The first occurred around the end of day 47 of 1978. The apparent failure mode involved a loose connection at the buck-out leading to a greatly enhanced

"noise" level, typically obscuring the plasma data (solar wind). The instrument was thermally cycled later in the year, leading to a "fix" on day 138 of 1978.

The instrument remained nominal throughout the Jupiter (March 1979) and Saturn (November 1980) encounters. The second failure occurred shortly after re-immersion into the solar wind after the Saturn encounter on day 328 of 1980. The second failure was qualitatively different from the first; in particular, the modulator voltage levels were greatly different and reversed in phase from what they should be during instrument operation.

Details of the failure circumstances, symptoms, and mode are given in *Voyager Memoranda 153: Failure of V1 Post Saturn.pdf*. There were repeated unsuccessful attempts to "recover" the instrument again via thermal cycling.

1.4 Data, Documentation, and Software: *Voyager_PLS_v_02/*

I have assembled most of the data from the mission, mostly in *ascii* format, but also in *binary* format (for example, the *Summary* and *edr* files for the mission are in binary). For those binary files I include, I have read routines for those files for *CentOS 7.9* and *Fedora 40* (see 1.4.2 below). "Data" includes both measurements from the instrument and the trajectory information for its position and orientation. I have put together a set of documentation explaining the various aspects of this assemblage and the mission. I have also included various software routines used to analyze the data, most importantly the program *mjsanl*, the program that performs the non-linear least-squares fits to ions with the full response of the instrument. Directions for and examples of the use of *mjsanl* are given in *MJSANL_v_02.*

Other useful computer routines are described in *VoyagerPLSUtilitySoftware_v_01.* All this material has been put into a folder in a directory named *Voyager_PLS_v_02*. Presently that directory is at

/nfs/faraday/data/jwb/Voyager_PLS_v_02

Flash drives containing this data and code and zip files of the data and code with an extraction script are also available.

The sub-directories of this main directory are as follows.

1.4.1 Voyager_PLS_v_02/documentation_v_02/

1.4.1.1 *Voyager_PLS_v_02/documentation_v_02/general*

This directory includes a *general* documentation directory, including this document, which will be referred to as *VI-PLS*, documentation on the *mjsanl* software (*MJSANL_v_02*) and other utility software routines (*VoyagerPLSUtilitySoftware_v_01*), and other relevant documents (Alan Barnett's thesis on the full response of the

instrument, a description of the program PMODEL by Vytenis Vasyliunas for the numerical computation of that response, and so on). The current contents are as follows:

Amador_2_peaks_senior_thesis.pdf: Senior thesis with examples of two peaked proton distributions.

16.2softwaredocs _Software library documentation_.pdf: From R. McNutt's collection of documentation, also in *Voyager_PLS_v_02/documentation_v_02/McNutt/Book 16 - Software dcoumentation/Book 16 - Software documentation*. I include it here as well because of its importance.

Ans_Array.pdf: The answer array for the positive ion mode, see *pranal.f*.
See *Voyager_PLS_v_02/software_v_01/historic_libraries/vgr_src_vgr/pranal.f.*

BarnettThesis.pdf: Alan Barnett's thesis.

Bevington.pdf: Bevington et al Data Reduction and Error Analysis for the Physical Sciences.

Butler (1989) [The Development and Construction of the Voyager Plasma Science Experiment, PLS; An Informal Historical Report].pdf

dnf_list_installed.txt: This is a list of the packages installed on my *Fedora release 38* running on my *X390 ThinkPad*. All the software routines discussed in this document run on this machine with this installation.

EDR_format_JPL.pdf: JPL document on the format of the Experimental Data Records (*edr*'s).

MJSANL_v_02.doc: Description of *mjsanl* in *Voyager_PLS_v_02/software_v_01/mjsanl*.
MJSANL_v_02.pdf: A pdf version of the above.

OgnnewNastov91PreFlightModulater.pdf

PMODEL.pdf: Documentation on VMV's simulation routine.

Positive ion fits near Europa.pdf: Output from the FULL UP MODE of *mjsanl*.

spl.pdf: George Gordon Jr.'s documentation on the *spl* files. The encounter data for all encounters was written in the *spl* binary format. See Section 7.5 below.
Summary_Tape_Format_Long.pdf: A longer version of the document below. The description of the positive ion answer array is complete I believe.

Summary_tape_format.pdf: GSFC documentation on the Summary tapes (see Section 7.6 below). The description of the positive ion answer array on page 1.15-5 is incomplete. The actual summary tape itself contains the full answer array (see Section 7.6 below).

vgranl.pdf: George Gordon Jr.'s memo on *VRGANL*, the automated analysis program for cruise which ran both at MIT and GSFC through 1989.

vgr.pdf: George Gordon Jr.'s memo on the Voyager mission files (also known as *vgr* files). See section 7.3 below.

Voyager Historical Data OCR - pages rotated.pdf: A memo from Ralph McNutt Jr. about the failure of the Voyager 1 instrument. Includes Voyager Memo 153, also available at *Voyager_PLS_v_02/documentation_v_02/voyager_memos/pdf/* .

VoyagerInterstellar_v_07.doc: A description of the Voyager PLS instrument and data (this document); *VoyagerInterstellar_v_07.pdf:* The pdf of this document.

VoyagerPLSUtilitySoftware_v_01.doc: Software routines for Voyager PLS.
VoyagerPLSUtilitySoftware_v_01.pdf: A pdf of the above document.

In addition, there is a folder named *var,* which contains documentation on a variety of routines, primarily written by George Gordon, Jr.

1.4.1.2 *Voyager_PLS_v_02/documentation_v_02/encounter_papers*

This directory contains published papers describing the six planetary encounters and the crossing of the termination shock and the heliopause.

1.4.1.3 *Voyager_PLS_v_02/documentation_v_02/publications*

A variety of publications, including Bridge's Space Science Review paper and Barnett and Olbert's article on the response function.

1.4.1.4 *Voyager_PLS_v_02/documentation_v_02/voyager_memos*

Voyager Memos document various issues around the data processing on Voyager, the encounter planning, definition of file formats, and so on. The first Voyager memo is dated June 2, 1977. There is then a long sequence through Voyager Memo 189, dated July 19, 1994, five years after the Neptune encounter. I have scanned all the Voyager Memos that I think are important, but not the complete set. These scanned memos are in *voyager_memos/pdf.*

Then, after a 23-year hiatus, the memos resume with Voyager Memo 190, dated November 10, 2017. This was after Voyager 2 crossed the termination shock (in 2007) but before it crossed into the interstellar medium (in 2018). The (current) last memo is Voyager Memo 217, dated April 22, 2023.

I will refer extensively to these memos in the following. In Section 9 below I give a listing of the entries in the *voyager_memos/pdf* directory. Note that word versions of the

more recent Voyager Memos (*VoyMemo_190_Processing_EDR_File.doc* through *VoyMemo_217_timing_problems_2023_107.doc*)
are in *voyager_memos/word_docs.*

1.4.2 Voyager_PLS_v_02/McNutt

Ralph McNutt Jr. kept extensive records for Voyager, which we include here. The documents are listed below (see also *Voyager Historical Data OCR - pages rotated.pdf* above):

3D Plots Jupiter
3D plots Saturn
Book 10 - Voyager 1 Side sensor data
Book 12 - Voyager 1 Side sensor data (Jupiter)
Book 13 - JPL 618-306 Appendices A, B, C
Book 14 - Subroutine writeups
Book 15 - SEDR Handbook
Book 16 - Software documentation
Book 17 - Jupiter spectra and fits, MJSANL and older
Book 18 - LABBI benchmarks
Book 19 - Voyager 2 data at Jupiter
Book 1 - Master writeups of VGRANL and MJSANL
Book 20 - Running Programs on the Sun Workstations
Book 2 - Voyager 2 M-modes
Book 3 - MJSANL Validation, Testing, Cost Analysis
Book 4 - Voyager 2 Jupiter L-mode spectra
Book 6 - CMS_VS1 Instructions, OIT memos, program and subroutine writeups
Book 8 - MJSANL and miscellaneous
Book 9 - Non-linear least squares fits to Voyager PLS data
Outer Planet Magnetospheres (folder) 1999-2000.pdf
README-Documentation.txt
s10 _Voyager Trajectory Information_.pdf
s1 _Galileansatellite encounters_.pdf
s2 _Voyager 2 encounter_ (with Jupiter).pdf
s3 _VGR 2 MAG 1979 180 - 1979 238_.pdf
s4 - Voyager 1 Fit Parameters.pdf
s5 - Voyager 2 Fit Parameters.pdf
s6 - Voyager 1 Encounter.pdf
s7 - Voyager 1 Fit Parameters w Saturated L modes.pdf
s8 - Voyager 1 Flux and Energy Plotes (24 Hr).pdf
s9 - Voyager 2 Flux and Energy Plots (24 Hr).pdf
Voyager 2 Neptune Encounter - PLS spectra and fits
Voyager PLS Mechanical and Assembly Drawings and Schematics

.

1.4.3 Voyager_PLS_v_02/software_v_01/

This directory contains a variety of software routines for Voyager data handling and analysis. Most importantly, *Voyager_PLS_v_02/software_v_01/* includes a directory */software_v_01/ mjsanl*, which contains a set of eighty-eight *Fortran .f* routines and 3 *.c* routines which perform our non-linear least-squares fits to ions. This set of programs compiles and runs on the MIT Kavli Institute's *CentOS 7.9*, linking to the data described below. It also runs on a Lenovo *X390* laptop running *Fedora release 40*. Their use is documented in *MJSANL_v_02,* see Section 1.4.1.1 above.

There are other sets of software in */software_v_01/* used for doing various tasks with the data, which are described in the document *VoyagerPLSUtilitySoftware_v_01.* All the software in this directory, except for one *idl* routine to produce spectrograms (see Section 7.4 below and Cases 9 and 10 of *The Voyager PLS Utility Software)*, runs on a Lenovo *X390* laptop (running *Fedora release 40*).

I have also included a directory *historic_libraries*, which includes most of the code used to run programs on *Solaris*. These routines are for reference, and they will not run on *CentOS.*

1.4.4 Voyager_PLS_v_02/v1/

Directory *v*1 includes Voyager 1 data and trajectory information, as follows:

calibrations:
The directory *calibration*s include a variety of calibrations from Voyager 1 over the mission from launch to its final failure (see Section 7.1 below).

cruise_ssedr:
The directory *cruise_ssedr* includes trajectory information for Voyager 1 over the cruise phase of the mission through its final failure (see Section 5.4 below).

daily_hourly_fine:
The directory *daily_hourly_fine* includes hourly average files for Voyager 1, and fine resolution data as well (see Section 7.2 below). There are no daily averages for Voyager 1.

encounter_spl:
The directory *encounter_spl* contains encounter data for Voyager 1 at Jupiter and Saturn (see Section 7.5 below).

encounter_ssedr
The directory *encounter_ssedr* contains trajectory data for Voyager 1 at Jupiter and Saturn (see Section 5.5 below).

spc

The directory *spc* contains cruise data in *data* and color spectrograms in *plots* for Voyager 1 (see Section 7.4 below) through 1980.

summary
The directory *summary* contains *Summary* files produced at GSFC for Voyager 1 through its final failure in 1980 after Saturn (see Section 7.6 below).

vgr
The directory *vgr* contains Mission files of cruise data for Voyager 1 through 1980 (see Section 7.3 below 1.5.2.3 above).

1.4.5 Voyager_PLS_v_02/v2/

Directory *v*2 is similar to *v1*, except there are four different planetary encounters for Voyager 2, instead of the two for Voyager 1. **Also, we have included a directory** *edr* which includes all the *edr* files after the *Summary* tape production at *GSFC* stopped, starting in 1990 and going up to the turn off. These are binary files, and there is a read routine for reading them in *Voyager_PLS_v_01/software_v_01/nxtedr_read*. Note that there is a significant gap of time (more than a year) between when the *summaries* stop and the *edr*s begin. We have data in this period (in both the *vgr* and *spc* format) but no calibrations, which were obtained from the *edr'*s after the *summary* tapes stopped.

Note also that the *Voyager_PLS_v_02/v2/vgr* directory only contains *vgr* (Mission) files through 2021.175.06. They stopped at this point because the cruise production on *Carrington* (Solaris) failed near this date, for unknown reasons, and we could no longer produce *vgr* files. Data beyond this point is available in *Voyager_PLS_v_02/v2/spc/data* through turn off.

1.4.6 Flash Drive for Transferring Data and Software (for MIT users only).

Here are the procedures I go through to transfer the data and software to a flash drive for general distribution.

Go to */nfs/faraday/data/jwb/Voyager_PLS_v_02*. When you are in this directory, an *"ls"* command will produce the following:

AAA_readme.txt
documentation_v_02
log_create_tar_files_at_MIT_10_10_2023
McNutt
reM
script_for_PLS_deploy
script_for_PLS_deploy_flashdrive
script_to_create_tar_files_for_Voyager_PLS_v_02
software_v_01
tar_files

v1
v2
Voyager_PLS_v_02.tar.gz
VOY_PLS_V02_readme.txt

For a totally fresh tar, make sure there is a sub-directory *tar_files* with only one file in it: *Voyager_PLS_v_02.tar.gz*. The file *Voyager_PLS_v_02.tar.gz* contains a skeleton directory structure for *Voyager_PLS_v_02* that I use for the install scripts. Then run the shell script *script_to_create_tar_files_for_Voyager_PLS_v_02*. The file *log_create_tar_files_at_MIT_10_10_2024* is a keyboard capture script for when I ran this script on October 10, 2024. This will produce 24 separate tar files of various parts of the directory *Voyager_PLS_v_02* and put them in the directory *tar_files*. It takes about 30 minutes to *tar* all the files. The size of the resultant *tar_files* directory is about 20 gigabytes.

When this script is finished running there should be 25 tar files in *tar_files*. Download this *tar_files* directory to a Windows machine, as well as the two scripts: *script_for_PLS_deploy* and *script_for_PLS_deploy_flashdrive*. Transfer this directory and the two scripts from the Windows machine to a flash drive named *VOY_PLS_V02*. Plug the flash drive into a *linux* machine running *Fedora 40*. Drag the two scripts and the directory *tar_files* to the directory on the *linux* machine where you want to install *Voyager_PLS_v_02*. Execute the script *script_for_PLS_deploy* (you may have to "chmod +x *script_for_PLS_deploy"* to make the script executable and also to execute type "./*script_for_PLS_deploy"*). This will *untar* all the tar files in *tar_files* into the directory structure on your *linux* machine that we describe in this document. The resultant directory *Voyager_PLS_v_02* is about 40 GB, and the *untar* process takes about 10 minutes on my *ThinkPad X390.*

If you also want ***to put back on your flash drive*** a copy of the unpacked files, execute the script *script_for_PLS_deploy_flashdrive* from your host *linux* computer, and that will untar *tar_files* into a directory *Voyager_PLS_v_02* on your original flash drive using commands like:

tar -xvf tar_files/software_v_01.tar.gz -C /run/media/jwbelcher/VOY_PLS_V01/Voyager_PLS_v_02

You must modify these commands to agree with your *linux* machine name (presumably not "*jwbelcher*"). It takes about 50 minutes to create this directory on *VOY_PLS_V02* on my *ThinkPad X390.*

1.5 An Informal History of the PLS Processing at MIT and GSFC

This is an informal overview of the processing of the data over the lifetime of the mission, based on my recollections. I am not familiar with a lot of the history, especially of *MJSANL*, and of the *vgr* or *spl* files, so what I describe below is my best guess about the production and evolution of these files.

1.5.1 Summary Tape Processing at *GSFC*

The Voyager 1 PLS and MAG processing were done conjointly at GSFC through Neptune (almost), using a package of programs called *vgranl*. I have included in *Voyager_PLS_v_02/software_v_01/historic_libraries/vgr_src_vgr* the programs that were used in that process. These are *Solaris* programs, and will not run on *CentOS*; I include them for reference.

I wrote the proton analysis routines used in *vgranl*, which included a moments estimate of the plasma parameters, and a non-linear least-squares fit based on those initial estimates (see Sections 3.1.3 and 3.2.4 below) assuming unit response for the sensors (see 3.2.3 below). The analysis produced an "*Answer Array*". The entries in the answer array are described in *documentation_v_02/general/Ans_Array.pdf*, *Summary_tape_format.pdf*, and *vgranl.pdf*, pages 41-50. Note that the list in *Summary_tape_format.pdf* is incomplete. There is also a description in

voyager_memos/pdf/VoyMemo_075_Voyager_Hourly_Average_Tapes.pdf,

and see also *VoyMemo_119_Corrected_Hourly_Average_Tape_Format.pdf*.

The *Summary* tapes were produced on Voyager 1 through the final failure of the instrument, and on Voyager 2 to just before the Neptune encounter: see *v2/summary/summary_85_89/ v2_sum_1989.230.19_1989.234.23.gz*. I am not sure why they do not include the Neptune encounter, but we have the data from other means, discussed below.

1.5.2 Production of Mission (*vgr*) files at *MIT*

At some point, George Gordon Jr.in the mid-1990s also started producing *Mission* or *vgr* files, whose format is described in the document *Voyager_PLS_v_02/documentation_v_02/general/vgr.pdf* (also see Section 7.3 below). This was after I stepped down as *PI* and John Richardson had become *PI*, sometime in the early 1990s. I do not remember discussing the creation of these files. I believe the motivation was to produce a set of files that were relatively small for reprocessing purposes. These files included all the digital current values, but only eleven variables from the answer array.

1.5.2.1 Millisecond Timing Issues on Mission files

The mission files have the feature that the time in milliseconds was truncated by dividing by 4 to make the format smaller and reconstituted afterward by multiplying by 4. This means that the times on the *vgr* files will differ from the times on other files at the millisecond level. An example is the time 1977 304 4 59 12 412 in Example 1 of the *MJSANL* document, which is a *vgr* time since *mjsanl* is reading *vgr* files for cruise analysis. The corresponding *correct* time on the summary tape for the same spectra is 1977 304 4 59 12 414). Note that ((414/4)*4 is 412. See *software_v_01/summary_pls_read/output*.

1.5.2.2 The Full Answer Array

The *vgr* files do not contain the full answer array, although presumably when they were produced in the MIT processing the full answer array was available. *As far as I know no record of the full answer array was kept in the vgr processing*, only the eleven elements mentioned above. The full answer array is available on the *summary* files for the times we have summary files, see *Voyager_PLS_v_02/v1/summary* and *Voyager_PLS_v_02/v2/summary*, and ***we can read*** PLS data from those files (see *software_v_01/summary_pls_read/* and Case 5 of *The Voyager PLS Utility Software*). But these files are only available on Voyager 2 until just before the Neptune encounter. Moreover, the full answer array from the *summary* tape for the one example I have compared does not agree with the corresponding eleven variables on the *vgr* files (see *software_v_01/summary_pls_read/output* compared to *software_v_01/mjsanl/example_01/script_01).* They are close but not the same. This leads me to believe that the *vgr* files have been processed again at MIT after the summary tape files were processed at *GSFC*, but I do not know that for sure.

1.5.2.3 Limitations of the Mission files

The *vgr* files have a complete set of data from the mission except for two important limitations.

The first is that they have only a partial set of the full data from the encounter modes at Uranus and Neptune. The encounters at these planets did not do a simple *E1, L, E2, M* sampling, as described in Section 3.3 below. A complete sampling sequence at Uranus and Neptune consisted of 50 measurements: 1 M long, 13 L longs, 6 E1 longs, 6 E2 longs, no M shorts, 12 L shorts, 6 E1 shorts, and 6 E2 shorts. "Long" is an integration time of 930 ms, "short" is an integration time of 21 ms. When George Gordon Jr came to produce the *vgr* files for these intervals, he did not include the full 50 mode measurement sequence, but only a simpler *E1, L, E2, M* sequence, including only one each of the *E1, L, E2* measurements. See *VoyMemo_202_Neptune_Data*, Table 1, and *VoyMemo_203_Uranus_Data*, Table 1, for a detailed explanation. Presumably this choice was made so that the format of the *vgr* files was the same across the mission. So, for the encounter periods at Uranus and Neptune, the *vgr* files only contain a subset of the total data (four of the 50 mode measurements in a cycle).

The second important limitation is that the *vgr* files were produced as standard output for the *vgranl* program running at MIT on a *Solaris* workstation, *Carrington*. That automated production failed on DOY 175 of 2021, and the last *vgr* file it produced was *v2_vgr_2021.001.03_2021.175.06* (see *Voyager_PLS_v_02/v2/vgr*). Note that *Carrington* did not have a hardware failure, it was the software that ceased to function, for unknown reasons. After that time the *vgranl Carrington* processing was replaced by a much simpler processing scheme, see for example

VoyMemo_215_Processing_EDRs__to_v2all_files_on_Faraday_v_02.pdf

that simply reads the *edr*'s and produces text files known as *v2all* files, containing only time and DN values, with no analysis, later reformatted into the *spc* files. See the file

VoyMemo_194_Archiving_Cruise_Spectral_Data.pdf

Between the *vgr* files and the *spc* files (see below), we have all the *DN* values for both spacecraft in *txt* files up to the turn off of the Voyager 2 instrument on September 27 2024.

1.5.2.4 *SPC* and *V1/2all files*

The production of the *v1all* and *v2all* files began in 2009 at my instigation, after the crossing of the termination shock, and they were updated to earlier times by Leslie Finck. My motivation was to get the currents in *ascii* format, since I was worried that in the long term, we would not be able to read the binary *vgr* files (this fear was unfounded: I have since written read routines for those binary files and converted them to *ascii,* see *VoyMemo_214_converting_VGR_files_from_binary_to_ascii.pdf*) . I also wanted color spectrograms over the mission, which were produced at the same time as the *v1/2all* files.

These files are what Leslie Finck produces today as the end of production (edr file as input, *v2all* file as output) and are where the *DN* data is stored since DOY 175 of 2021 after the failure of the standard production (see 1.5.2.3 above). These v2all files are quite large, but they contain all the data up to the turn off. I use those files to make a much smaller file containing the same information called the *spc* files, which is what I include in this collection of data, found at *Voyager_PLS_v_02/v1/spc* and *Voyager_PLS_v_02/v2/spc* (see Section 7.4 below). My program to take a *v2all* file and make a *spc* file can be found at *software_v_01/spc_file_from_v12all_file*, see also Case 8 of *The Voyager PLS Utility Software.*

1.5.3 *SPL* files for the encounters

At some point that I am not aware of, we started producing *SPL* files for the encounters. See the document *Voyager_PLS_v_02/documentation_v_02/general/spl.pdf*.
I do not remember discussing the creation of these files. I have no idea of the provenance of these files, that is did they come from the summary files from *GSFC* or were they made internally at MIT from *edr* files. I was not even aware that such files existed until Fran Bagenal's *PDART* program began in 2021. Their format is described in the memo above and

VoyMemo_193_Converting_Encounter_SPL_Files_to_Text_files.pdf

These were binary files, and for each encounter there were many partial files scattered on the MIT computers. After an extended effort as part of Fran Bagenal's PDART grant, I assembled a combined set of all the *spl* files we could find for each encounter, as described in the following memos:

VoyMemo_202_Neptune_Data.pdf

VoyMemo_203_Uranus_Data.pdf
VoyMemo_204_v2_Saturn_Data_v_02.pdf
VoyMemo_205_v2_Jupiter_Data_v_03.pdf
VoyMemo_206_v1_Jupiter_Data_v_02.pdf
VoyMemo_207_v1_Saturn_Data.pdf

These data are contained in an *ascii* format in *Voyager_PLS_v_02/v1/encounter_spl* and *Voyager_PLS_v_02/v2/encounter_spl.*

1.5.4 The Full Response Function and *MJSANL*

A major advance in the analysis of PLS data came with the development of the full response function of the instrument by Barnet and Olbert (see *documentation_v_01/publications/BarnettOlbert1986.pdf*). The motivation for this development was the analysis of the PLS data near the Io Flux Tube, where the flow is oblique and required the full response to analyze. Subsequently, Ralph McNutt Jr. and colleagues put together the *MJSANL* program, which was used at all the magnetospheres to analyze data. Fran Bagenal has reproduced this code at Colorado in *idl*. We give examples of the use of this code at all the magnetospheres, the heliosheath, and the solar wind in *MJSANL: The Positive-Ion Least-Squares Fitting Routine for the Voyager PLS Instrument.*

2 Spacecraft and *PLS* Instrument

2.1 Configuration

The Plasma Science Experiment (PLS) is shown below. The various cups in the main sensor (A, B, C) have normals which make an angle of 20 degrees to the symmetry axis of the main sensor, which is aligned with the $-Z_{s/c}$ axis.

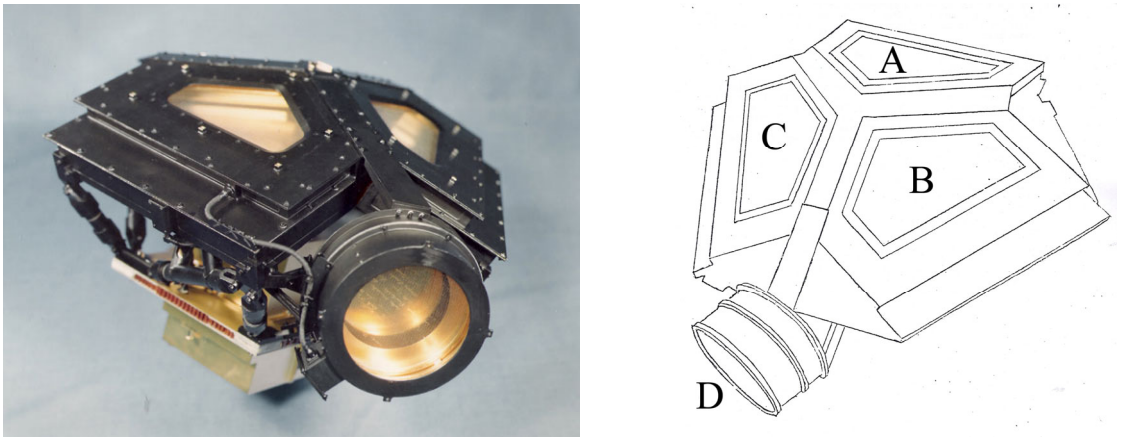

Figure 2.1-1: The four sensors of the Plasma Science Experiment

The experiment is mounted on the science boom, as shown in the figures below.

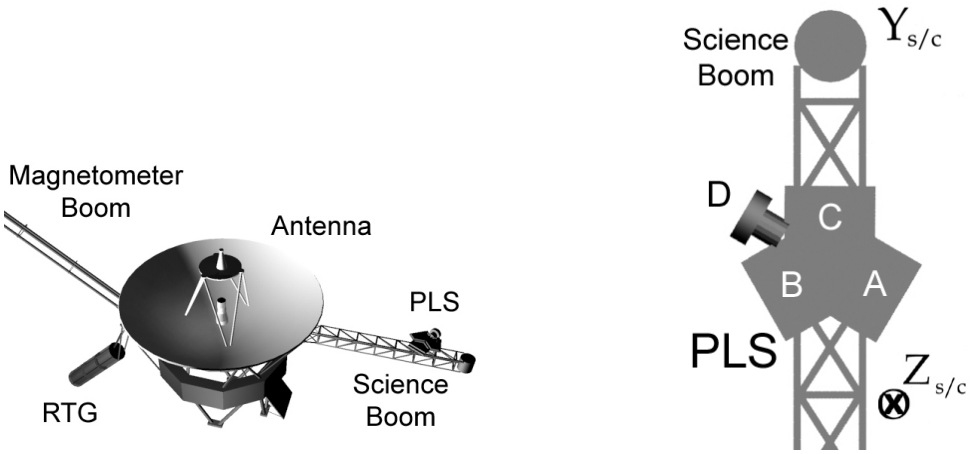

Figure 2.1-2: The Voyager Spacecraft and a close-up of the science boom.

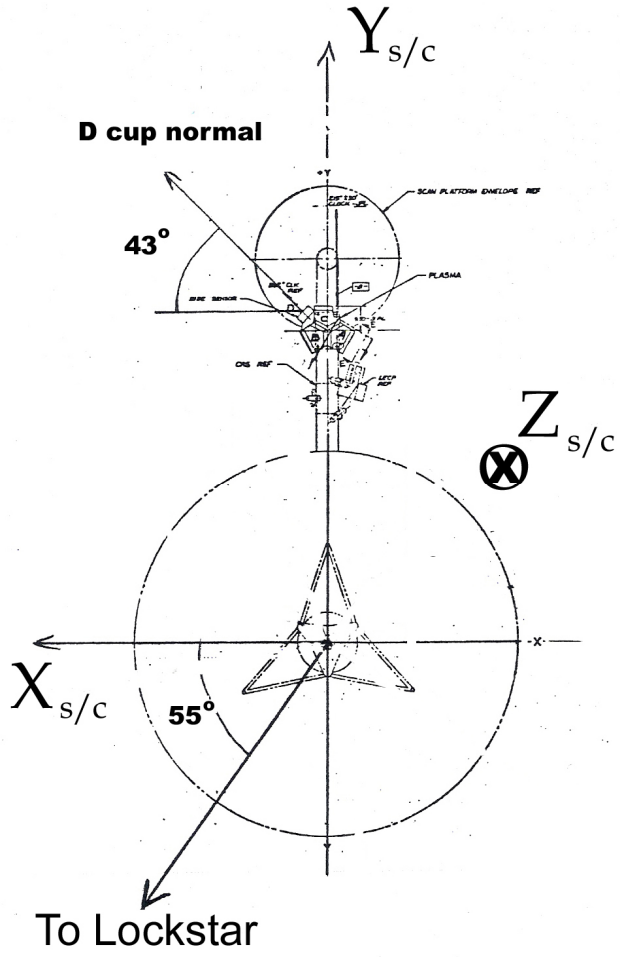

Figure 2.1-3: Spacecraft Coordinates

2.2 Spacecraft coordinates and cup normals

The symmetry axis of the main PLS cluster is along the negative spacecraft Z axis (see Figures 2.1-2 and 2.1-3), which is aligned with the spacecraft antenna. When the spacecraft antenna is pointed at the earth (the usual configuration), the negative spacecraft Z axis points toward the earth, as does the symmetry axis of the main PLS cluster. The definition of the spacecraft axes are shown in Figure 2.1-3. The various cup normals of the four plasma sensors in spacecraft coordinates are given by

$$\hat{\mathbf{n}}_A = -\hat{\mathbf{X}}_{s/c}\sin 20^\circ \cos 30^\circ - \hat{\mathbf{Y}}_{s/c}\sin 20^\circ \cos 60^\circ - \hat{\mathbf{Z}}_{s/c}\cos 20^\circ \tag{2.2.1}$$

$$\hat{\mathbf{n}}_B = \hat{\mathbf{X}}_{s/c}\sin 20^\circ \cos 30^\circ - \hat{\mathbf{Y}}_{s/c}\sin 20^\circ \cos 60^\circ - \hat{\mathbf{Z}}_{s/c}\cos 20^\circ \tag{2.2.2}$$

$$\hat{\mathbf{n}}_C = \hat{\mathbf{Y}}_{s/c}\sin 20^\circ - \hat{\mathbf{Z}}_{s/c}\cos 20^\circ \tag{2.2.3}$$

$$\hat{\mathbf{n}}_D = \hat{\mathbf{X}}_{s/c}\cos 43^\circ + \hat{\mathbf{Y}}_{s/c}\sin 43^\circ \tag{2.2.4}$$

We can invert this non-orthogonal transformation to obtain

$$\hat{\mathbf{X}}_{s/c} = \frac{\hat{\mathbf{n}}_B - \hat{\mathbf{n}}_A}{2\sin 20 \cos 30} \tag{2.2.5}$$

$$\hat{\mathbf{Y}}_{s/c} = \frac{1}{\sin 20^\circ \left(1+\cos 60^\circ\right)}\left[\hat{\mathbf{n}}_C - \frac{\hat{\mathbf{n}}_A + \hat{\mathbf{n}}_B}{2}\right] \tag{2.2.6}$$

$$\hat{\mathbf{Z}}_{s/c} = -\left[\frac{\hat{\mathbf{n}}_A + \hat{\mathbf{n}}_B}{2\cos 60^\circ} + \hat{\mathbf{n}}_C\right]\left[\frac{\cos 60^\circ}{\cos 20^\circ \left(1+\cos 60^\circ\right)}\right] \tag{2.2.7}$$

When in the supersonic solar wind, the various cups in the main sensor measure the components of proton velocity *along the direction anti-parallel to the sensor normal*, so if V_A, V_B, and V_C are the measured components of the solar wind speed along the cup normals, they are related to the solar wind components in spacecraft coordinates by

$$V_A = V_{X\,s/c}\sin 20^\circ \cos 30^\circ + V_{Y\,s/c}\sin 20^\circ \cos 60^\circ + V_{Z\,s/c}\cos 20^\circ \tag{2.2.8}$$

$$V_B = -V_{X\,s/c}\sin 20^\circ \cos 30^\circ + V_{Y\,s/c}\sin 20^\circ \cos 60^\circ + V_{Z\,s/c}\cos 20^\circ \tag{2.2.9}$$

$$V_C = -V_{Y\,s/c}\sin 20^\circ + V_{Z\,s/c}\cos 20^\circ \tag{2.2.10}$$

and conversely

$$V_X = \frac{V_A - V_B}{2\sin 20 \cos 30} \tag{2.2.11}$$

$$V_Y = \frac{1}{\sin 20^\circ \left(1+\cos 60^\circ\right)}\left[-V_C + \frac{V_A + V_B}{2}\right] \tag{2.2.12}$$

$$V_Z = \left[\frac{\cos 60^\circ}{\cos 20^\circ \left(1+\cos 60^\circ\right)}\right]\left[\frac{V_A + V_B}{2\cos 60^\circ} + V_C\right] \tag{2.2.13}$$

Numerically, the cup normals have the following values

	Xs/c	Ys/c	Zs/c
A cup	-0.296198	-0.171010	-0.939693
B cup	0.296198	-0.171010	-0.939693
C cup	0.000000	0.342020	-0.939693
D cup	0.731354	0.681998	0.000000

(2.2.14)

2.3 The Canopus Sensor

Consider a spherical polar coordinate system based on spacecraft coordinates. The Canopus sensor is a slit which is narrow in azimuth in this system. The narrow azimuth extent of the slit is centered at -55 degrees in azimuth (see Figure 2.1-3 above). The slit is elongated in the polar angle, with the center of the elongated slit at a polar angle of 90 degrees (that is, in the $X_{s/c}$-$Y_{s/c}$ plane). When the Canopus sensor is on a given lock star, the direction to that star will lie somewhere in a plane perpendicular to the $X_{s/c}$-$Y_{s/c}$ plane with an azimuth angle of -55 degrees, as indicated in Figure 2.1-3.

3 Instrument

A full description of the instrument is given in Bridge, H. S., J. W. Belcher, R. J. Butler, A. J. Lazarus, A. Mavretic, G. L. Siscoe, J. D. Sullivan, and V. M. Vasyliunas: The Plasma Experiment on the 1977 Voyager Mission, *Space Science Reviews*, **21**, 259-287, 1977. This article can be found at (see Section 1.4.1.4 above)

documentation_v_02/publications/Bridge_space_science_review.pdf

3.1 The Experimental Concept

The Voyager measurement concept for a supersonic plasma such as the solar wind provides: (1) complete coverage of phase space with high time resolution; (2) determination of the density, velocity, pressure tensor, and heat flux, with no model assumptions; (3) ease of data interpretation—that is the above properties can be obtained by the formation of sums based directly on the measured currents; (4) ease of a non-linear least squares fit analysis if desired.

These features are achieved with the use of a cluster of three modulated grid Faraday cup plasma detectors (Figure 2.1-1). The axis of symmetry of the cluster (the spacecraft $-\hat{\mathbf{z}}$ direction) is approximately along the spacecraft-earth line, which is close to the spacecraft-sun line. The normal to each of the three cups (referred to as the A, B, and C detectors) are each 20 degrees from the symmetry axis and 120 degrees apart in azimuth. Each detector has an extremely wide field of view for full acceptance of the incident plasma ions, and the cluster has a common field of view which is a cone of approximately 45 degrees half-angle about the symmetry axis. All the main detectors have full acceptance in this common field of view.

3.1.1 Voltage Levels

3.1.1.1 *L-Mode*

Let Φ_k be the lower modulator voltage for the k-th energy window (*k* runs from 1 to 16 for the *L* (low resolution) ion mode and from 1 to 128 for the *M* (high resolution) ion mode. Then for the *L* mode, these lower (upper) voltage in channel k (k-1) are given by

$$\Phi_k = \left[60\left(1.33352\right)^{k-1} - 50 \right] \text{ Volts} \quad k = 1 \text{ to } 17 \tag{3.1.1.1}$$

and in the *M* mode by

$$\Phi_k = \left[60\left(1.03663\right)^{k-1} - 50 \right] \text{ Volts} \quad k = 1 \text{ to } 129 \tag{3.1.1.2}$$

Table 3-1 shows the various voltages and speeds in the *L* mode.

channel	Lower voltage	Lower speed	Average Speed	Delta Speed
1	10.0	43.8	59.8	32.1
2	30.0	75.8	90.0	28.4
3	56.7	104.2	118.6	28.7
4	92.3	133.0	148.3	30.7
5	139.7	163.6	180.4	33.6
6	203.0	197.2	215.9	37.4
7	287.4	234.7	255.7	42.2
8	399.9	276.8	300.7	47.8
9	550.0	324.6	351.9	54.5
10	750.1	379.1	410.3	62.3
11	1017.0	441.4	477.1	71.4
12	1372.8	512.9	553.9	82.1
13	1847.3	594.9	642.1	94.4
14	2480.1	689.3	743.7	108.7
15	3324.0	798.0	860.7	125.3
16	4449.3	923.3	995.5	144.4
17	5949.9	1067.7		

Table 3-1: Voltages and speeds for the *L mode*

In Table 3-1, a given voltage Φ_k corresponds to a proton speed given by

$$\tfrac{1}{2} m_{proton} \mathrm{v}_k^2 = q_{proton} \Phi_k \quad \text{or} \quad \mathrm{v}_k = \sqrt{\frac{2 q_{proton} \Phi_k}{m_{proton}}} = 13.8418 \sqrt{\Phi_k} \tag{3.1.1.3}$$

where in the last equation, if Φ_k is given in volts, then the speed is in km/s.

3.1.1.2 *M-Mode*

Table 3-2 shows the various voltages and speeds in the *M* mode, with the same quantities as in Table 3-1.

Channel	Lower Φ_k	Lower v_k	Ave v_k	Delta v_k
1	10.0	43.8	46.1	4.57
2	12.2	48.3	50.5	4.32
3	14.5	52.7	54.7	4.13
4	16.8	56.8	58.8	3.99
5	19.3	60.8	62.7	3.88
6	21.8	64.7	66.6	3.79
7	24.5	68.5	70.3	3.72
8	27.2	72.2	74.0	3.66
9	30.0	75.8	77.6	3.62
10	32.9	79.4	81.2	3.58
11	36.0	83.0	84.8	3.56
12	39.1	86.6	88.4	3.54
13	42.4	90.1	91.9	3.53
14	45.8	93.7	95.4	3.52
15	49.3	97.2	98.9	3.52
16	52.9	100.7	102.5	3.52
17	56.7	104.2	106.0	3.53
18	60.6	107.8	109.5	3.54
19	64.7	111.3	113.1	3.56
20	68.9	114.9	116.6	3.58
21	73.2	118.4	120.2	3.60
22	77.7	122.0	123.8	3.62
23	82.4	125.6	127.5	3.64
24	87.2	129.3	131.1	3.67

Channel	Lower Φ_k	Lower v_k	Ave v_k	Delta v_k
25	92.3	133.0	134.8	3.70
26	97.5	136.7	138.5	3.74
27	102.9	140.4	142.3	3.77
28	108.5	144.2	146.1	3.81
29	114.3	148.0	149.9	3.85
30	120.3	151.8	153.8	3.89
31	126.5	155.7	157.7	3.93
32	133.0	159.6	161.6	3.97
33	139.7	163.6	165.6	4.02
34	146.7	167.6	169.7	4.07
35	153.9	171.7	173.8	4.12
36	161.3	175.8	177.9	4.17
37	169.1	180.0	182.1	4.22

38	177.1	184.2	186.3	4.28
39	185.4	188.5	190.7	4.33
40	194.0	192.8	195.0	4.39
41	203.0	197.2	199.4	4.45
42	212.3	201.7	203.9	4.51
43	221.9	206.2	208.5	4.58
44	231.8	210.8	213.1	4.64
45	242.1	215.4	217.7	4.71
46	252.8	220.1	222.5	4.78
47	263.9	224.9	227.3	4.85
48	275.4	229.7	232.2	4.92
49	287.4	234.6	237.1	4.99
50	299.7	239.6	242.2	5.07
51	312.5	244.7	247.3	5.14
52	325.8	249.8	252.5	5.22
53	339.6	255.1	257.7	5.30
54	353.8	260.4	263.1	5.39
55	368.6	265.8	268.5	5.47
56	384.0	271.2	274.0	5.56
57	399.9	276.8	279.6	5.65
58	416.3	282.4	285.3	5.74
59	433.4	288.2	291.1	5.83

Channel	Lower Φ_k	Lower v_k	Ave v_k	Delta v_k
60	451.1	294.0	297.0	5.92
61	469.5	299.9	302.9	6.02
62	488.5	305.9	309.0	6.12
63	508.2	312.1	315.2	6.22
64	528.7	318.3	321.4	6.32
65	549.9	324.6	327.8	6.42
66	571.9	331.0	334.3	6.53
67	594.6	337.5	340.9	6.64
68	618.3	344.2	347.5	6.75
69	642.7	350.9	354.4	6.86
70	668.1	357.8	361.3	6.98
71	694.4	364.8	368.3	7.09
72	721.7	371.8	375.5	7.21
73	750.0	379.1	382.7	7.33
74	779.3	386.4	390.1	7.46
75	809.6	393.9	397.6	7.59
76	841.1	401.4	405.3	7.72
77	873.8	409.2	413.1	7.85
78	907.6	417.0	421.0	7.98
79	942.7	425.0	429.0	8.12
80	979.0	433.1	437.2	8.26
81	1016.7	441.4	445.6	8.40

82	1055.8	449.8	454.0	8.55
83	1096.3	458.3	462.7	8.69
84	1138.3	467.0	471.4	8.85
85	1181.8	475.8	480.3	9.00
86	1226.9	484.8	489.4	9.16
87	1273.7	494.0	498.7	9.32
88	1322.2	503.3	508.1	9.48
89	1372.5	512.8	517.6	9.64
90	1424.6	522.4	527.3	9.81
91	1478.6	532.3	537.2	9.98
92	1534.6	542.2	547.3	10.16
93	1592.6	552.4	557.6	10.34
94	1652.8	562.7	568.0	10.52
95	1715.2	573.3	578.6	10.71
96	1779.8	584.0	589.4	10.89
97	1846.9	594.9	600.4	11.09
98	1916.3	605.9	611.6	11.28
99	1988.4	617.2	623.0	11.48
100	2063.0	628.7	634.5	11.69
101	2140.4	640.4	646.3	11.89
102	2220.7	652.3	658.3	12.10
103	2303.8	664.4	670.5	12.32
104	2390.1	676.7	683.0	12.54
105	2479.4	689.2	695.6	12.76
106	2572.1	702.0	708.5	12.99
107	2668.1	715.0	721.6	13.22

Channel	Lower Φ_k	Lower v_k	Ave v_k	Delta v_k
108	2767.7	728.2	734.9	13.45
109	2870.9	741.7	748.5	13.69
110	2977.9	755.3	762.3	13.94
111	3088.8	769.3	776.4	14.19
112	3203.8	783.5	790.7	14.44
113	3323.0	797.9	805.3	14.70
114	3446.5	812.6	820.1	14.96
115	3574.6	827.6	835.2	15.23
116	3707.4	842.8	850.6	15.50
117	3845.0	858.3	866.2	15.78
118	3987.7	874.1	882.1	16.06
119	4135.6	890.1	898.3	16.35
120	4288.9	906.5	914.8	16.64
121	4447.8	923.1	931.6	16.94
122	4612.6	940.1	948.7	17.25
123	4783.4	957.3	966.1	17.56
124	4960.4	974.9	983.8	17.87
125	5144.0	992.8	1001.9	18.19

126	5334.2	1010.9	1020.2	18.52
127	5531.4	1029.5	1038.9	18.85
128	5735.9	1048.3	1057.9	19.19
129	5947.8	1067.5	0.0	0.00

Table 3-2: Voltages and speeds for the *M mode*

3.1.2 Reduced Distribution Function and Measured Currents

To understand the Voyager moments calculation, let $\hat{\mathbf{n}}$ be the unit normal to a given collector, and $\hat{\mathbf{t}}_1$ and $\hat{\mathbf{t}}_2$ be mutually perpendicular unit vectors which are transverse to $\hat{\mathbf{n}}$. Let A be the area of the sensor, and q_{proton} the charge on a proton. If v_k is the lower speed for the k-th energy channel, then the modulated current I_k measured by the Faraday cup for the *k-th* channel is related to the particle distribution function $f(\mathbf{v})$ by:

$$I_k = q_{proton} A \int_{v_k}^{v_{k+1}} dv_n v_n \int_{-\infty}^{\infty}\int_{-\infty}^{\infty} dv_{t1} dv_{t2} f(\mathbf{v}) G(\mathbf{v}, \hat{\mathbf{n}}) \qquad (3.1.2.1)$$

In this expression $f(\mathbf{v})$ is the distribution function, $G(\mathbf{v}, \hat{\mathbf{n}})$ is the fraction of the aperture that intercepts the collector when projected in a given direction $\mathbf{v}$, and (v_n, v_{t1}, v_{t2}) are the components of the velocity along ($\hat{\mathbf{n}}, \hat{\mathbf{t}}_1, \hat{\mathbf{t}}_2$). The three cups in the main cluster have been designed to have wide fields of view, so that in the solar wind, the function $G(\mathbf{v}, \hat{\mathbf{n}})$ in equation (3.1.2.1) can be taken to be simply the transparency of the grids for all reasonable angles of incidence of the solar wind.

In the planetary magnetospheres, the heliosheath, and the interstellar medium, we cannot make this approximation, and analysis of the data requires the use of the full response function of the instrument (see *documentation_v_02/publications/BarnettOlbert1986.pdf* and the examples given in *documentation_v_02/general/MJSANL_v_02.pdf*).

In addition, in the inner solar system the thermal speed of the solar wind protons is much greater than the width of the channels in speed, as the velocity windows are narrow ($\Delta v / v \approx 1.8\%$), so that in equation (3.1.2.1) it is reasonable to assume that the distribution function is only slowly varying over a channel. With this assumption, and defining the average and difference speeds for a given channel as

$$\overline{v}_k = (v_{k+1} + v_k)/2 \qquad \Delta v_k = (v_{k+1} - v_k) \qquad (3.1.2.2)$$

we can write equation (3.1.2.1) as

$$I_k = q_{proton} A_{eff} \Delta v_k \overline{v}_k \int_{-\infty}^{\infty}\int_{-\infty}^{\infty} dv_{t1} dv_{t2} f(\overline{v}_k, v_{t1}, v_{t2}) \qquad (3.1.2.3)$$

where A_{eff} is the product of the area of the cups and the transparency of the grids. Let us define the reduced distribution function F as

$$F(\mathrm{v}_n) = \int_{-\infty}^{\infty}\int_{-\infty}^{\infty} d\mathrm{v}_{t1} d\mathrm{v}_{t2} f\left(\mathrm{v}_n, \mathrm{v}_{t1}, \mathrm{v}_{t2}\right) \tag{3.1.2.4}$$

From the above equations, a good estimate of F evaluated at $\overline{\mathrm{v}}_k$ is

$$F(\mathrm{v}_n)\big|_{\mathrm{v}_n=\overline{\mathrm{v}}_k} = I_k / \left[q_{proton} A_{eff} \Delta \mathrm{v}_k \overline{\mathrm{v}}_k \right] \tag{3.1.2.5}$$

3.1.3 Moments Calculation

The direct connection between the measured currents and the reduced distribution function shown in equation (3.1.2.5) is the key to the simplicity of the Voyager data analysis in the warm, supersonic solar wind. Each detector samples the full distribution function in a manner which is differential for the velocity component parallel to the detector normal and integral for the velocity components perpendicular to the detector normal. The cluster provides measurements of the reduced distribution function in each of three reasonably well separated directions. This information can be used to obtain the moments of the full distribution function *f*, given the magnetic field direction, in a straightforward manner, as follows.

The definition of the moments of *f* through the third moment are given by

$$N = \iiint f \, d^3\mathrm{v} \tag{3.1.3.1}$$

$$\mathbf{V} = \iiint \mathbf{v} f \, d^3\mathrm{v} / N \tag{3.1.3.2}$$

$$\vec{\vec{\mathbf{P}}} = m \iiint (\mathbf{v}-\mathbf{V})(\mathbf{v}-\mathbf{V}) f \, d^3\mathrm{v} \tag{3.1.3.3}$$

$$\vec{\vec{\mathbf{Q}}} = \tfrac{1}{2} m \iiint (\mathbf{v}-\mathbf{V})(\mathbf{v}-\mathbf{V})(\mathbf{v}-\mathbf{V}) f \, d^3\mathrm{v} \tag{3.1.3.4}$$

where $\vec{\vec{\mathbf{P}}}$ is the second rank pressure tensor and $\vec{\vec{\mathbf{Q}}}$ is the third rank heat flux tensor. If we assume that f is gyro-tropic, then we can write

$$\vec{\vec{\mathbf{P}}} = (P_{\parallel} - P_{\perp}) \hat{\mathbf{b}}\hat{\mathbf{b}} + P_{\perp} \vec{\vec{\mathbf{I}}} \tag{3.1.3.5}$$

$$\vec{\vec{\mathbf{Q}}} = Q_{\parallel} \hat{\mathbf{b}}\hat{\mathbf{b}}\hat{\mathbf{b}} + Q_{\perp} \vec{\vec{\mathbf{I}}}\,\hat{\mathbf{b}} \tag{3.1.3.6}$$

where $\hat{\mathbf{b}}$ is the unit vector along the magnetic field direction.

Consider a given detector with normal $\hat{\mathbf{n}}$. Let θ_n be the angle between the magnetic field direction and the cup normal. We can calculate the moments of *F* by approximating integrals by sums. From the equations above, for each cup we can find the following moments of *F*.

$$N = \int F(\mathrm{v}_n)\, d\mathrm{v}_n = \sum_k \left[\frac{I_k}{q_{proton} A_{eff} \Delta \mathrm{v}_k \overline{\mathrm{v}}_k} \right] \Delta \mathrm{v}_k = \frac{1}{q_{proton} A_{eff}} \sum_k \left[\frac{I_k}{\overline{\mathrm{v}}_k} \right] \tag{3.1.3.7}$$

$$V_n = \int \mathrm{v}_n F(\mathrm{v}_n)\, d\mathrm{v}_n / N = \sum_k \overline{\mathrm{v}}_k \left[\frac{I_k}{q_{proton} N A_{eff} \Delta \mathrm{v}_k \overline{\mathrm{v}}_k} \right] \Delta \mathrm{v}_k = \frac{1}{q_{proton} N A_{eff}} \sum_k [I_k] \tag{3.1.3.8}$$

$$\begin{aligned} P_{nn} &= \hat{\mathbf{n}} \cdot \vec{\vec{\mathbf{P}}} \cdot \hat{\mathbf{n}} = P_{\parallel} \cos^2 \theta_n + P_{\perp} \sin^2 \theta \\ &= m \int (\mathrm{v}_n - \mathrm{V}_n)^2 F(\mathrm{v}_n)\, d\mathrm{v}_n = \frac{m}{q_{proton} A_{eff}} \sum_k (\overline{\mathrm{v}}_k - \mathrm{V}_n)^2 \left[\frac{I_k}{\overline{\mathrm{v}}_k} \right] \end{aligned} \tag{3.1.3.9}$$

$$\begin{aligned} Q_{nnn} &= Q_{\parallel} \cos^3 \theta_n + 3 Q_{\perp} \cos \theta_n \\ &= \frac{m}{2} \int (\mathrm{v}_n - \mathrm{V}_n)^3 F(\mathrm{v}_n)\, d\mathrm{v}_n = \frac{m}{2 q_{proton} A_{eff}} \sum_k (\overline{\mathrm{v}}_k - \mathrm{V}_n)^3 \left[\frac{I_k}{\overline{\mathrm{v}}_k} \right] \end{aligned} \tag{3.1.3.10}$$

Each of these equations is repeated for each of the three cups. Thus, knowledge of the field direction and the moments of the three reduced distribution functions is sufficient to determine *N* (three independent estimates), **V**, $P_{\parallel}$ and $P_{\perp}$ (over-determined), and $Q_{\parallel}$ and $Q_{\perp}$ (over-determined). The sums indicated in the equations above are carried out by the Fortran routine *moments.f* (see Section 4.4 below).

3.1.4 Relationship between Pressure, Temperature, and Thermal Speed

To calculate a thermal speed W_{nn}, we have the following relationships:

$$P_{nn} = N k T_{nn} = N \left[\tfrac{1}{2} m W_{nn}^2 \right] \qquad W_{nn} = \sqrt{\frac{2 P_{nn}}{m N}} \qquad T_{nn} = \frac{\tfrac{1}{2} m W_{nn}^2}{k} \qquad W_{nn} = \sqrt{\frac{2 k T_{nn}}{m}} \tag{3.1.4.1}$$

Comparing (3.1.4.1) with (3.1.3.9), we see that

$$W_{nn} = \sqrt{2 \int (\mathrm{v}_n - \mathrm{V}_n)^2 F(\mathrm{v}_n)\, d\mathrm{v}_n / N} = \sqrt{\frac{2}{q_{proton} N A_{eff}} \sum_k (\overline{\mathrm{v}}_k - \mathrm{V}_n)^2 \left[\frac{I_k}{\overline{\mathrm{v}}_k} \right]} \tag{3.1.4.2}$$

3.1.5 Theoretical Examples of the Voyager Measurement Scheme

To illustrate this scheme with two concrete examples, we show in Figure 3.1-1 and Figure 3.1-2 two different samples of the same distribution function. The distribution function consists of two bi-Maxwellians, with one hotter than the other. In each case, the bottom panel of the figure shows iso-density contours of the distribution function. For ease of presentation, we have assumed that the bulk velocity **V**, the magnetic field **B**, and a given cup normal $\hat{\mathbf{n}}$ all lie in the plane of the paper.

Also indicated in the lower panel is the way a given detector slices the distribution function for a given $\hat{\mathbf{n}}$. In the upper panel we show the measured currents which would result from this sampling for a given $\hat{\mathbf{n}}$. Note the difference between the measured currents in the case when $\hat{\mathbf{n}}$ has a large projection along **B** (Figure 3.1-1) as contrasted to the case when $\hat{\mathbf{n}}$ has a small projection along **B** (Figure 3.1-2). Although over-idealized, these figures clearly illustrate in principle the three-dimensional capabilities of the Voyager measurements.

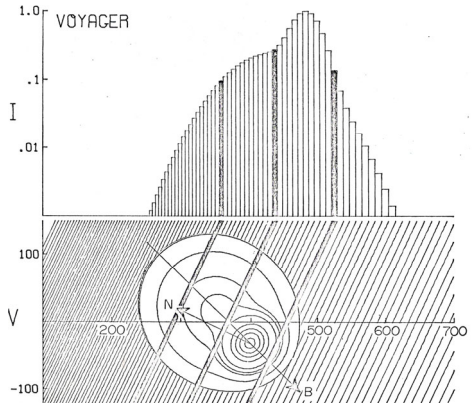

Figure 3.1-1: Theoretical currents, B and $\hat{\mathbf{n}}$ close to parallel.

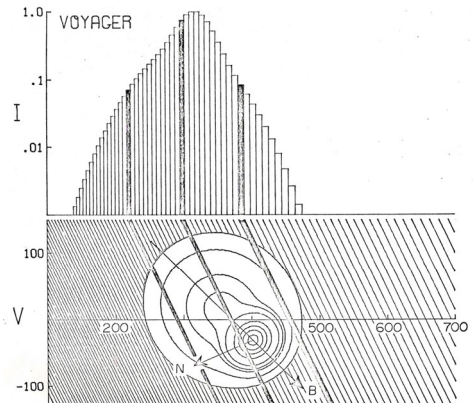

Figure 3.1-2: Theoretical currents, B and $\hat{\mathbf{n}}$ close to perpendicular.

3.2 Measured Voyager Ion Spectra

3.2.1 Solar Wind M Modes

Figure 3.2-1 shows four sample spectra from the M mode sequence from early in the mission. Measured currents (fluxes) in each of the three detectors are indicated by the step-like lines. On each figure, we also give some of the results of the moment calcu1ations for the proton peak. In two of the figures, least squares fit points using Maxwellians are indicated by crosses and diamonds. The instrument quantizes the currents logarithmically using eight bits to cover a range of four decades for each gain state of the instrument. The quantization error is thus + 1.8%. The noise level is equal to 6×10^{-14} amps for the integration time used in the measurements presented here. At the highest bit rate, an *M* mode spectrum is obtained every twelve seconds (see Section 3.6.2 below) For the alpha particle distribution, the peak is located at twice the energy of the proton peak in all detectors, because we are measuring energy per charge and an alpha particle moving at the same speed as a proton has twice the energy per charge (four times the mass and twice the charge).

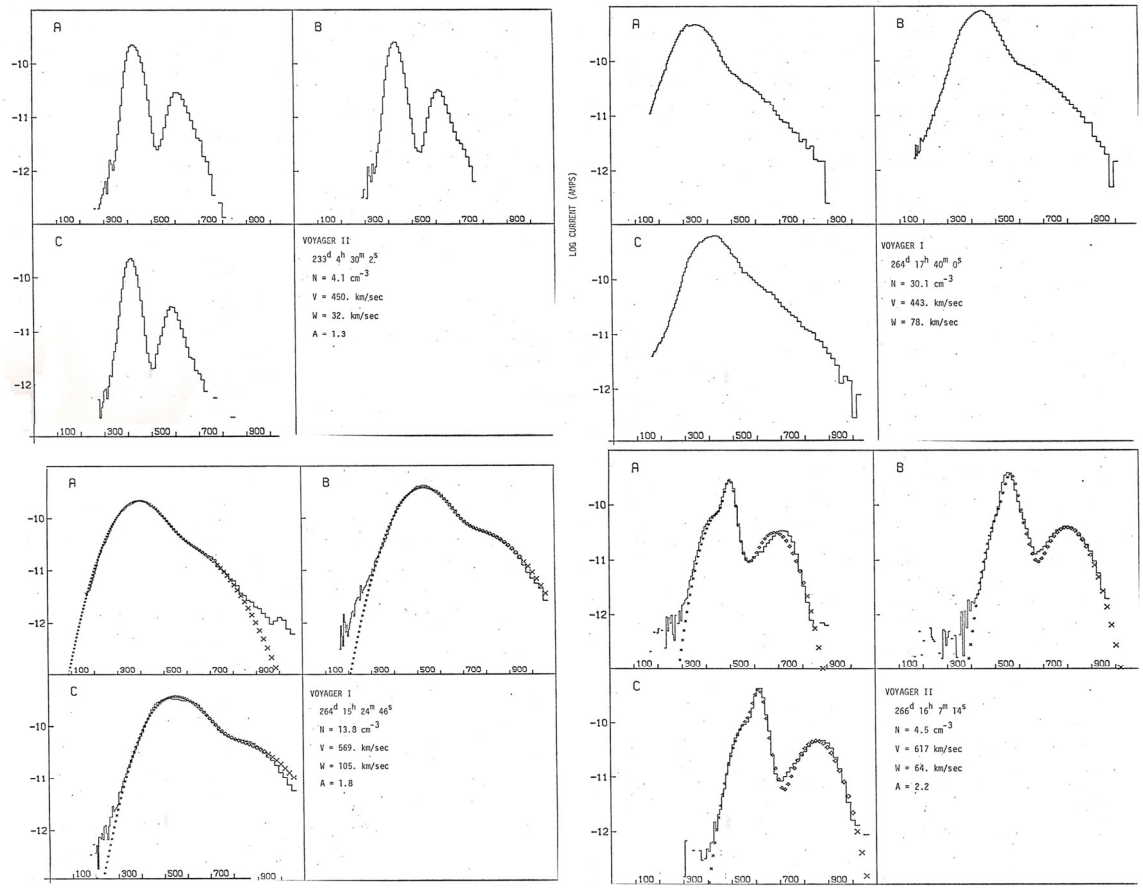

Figure 3.2-1: Four Examples of Measured Ion Currents in the M Mode

3.2.2 Heliosheath L Modes

Voyager 2 crossed the termination shock in August of 2007. Figure 3.2-2 shows a heliosheath spectra and least squares fit at the time indicated. Fit parameters are given at the bottom of the Figure. The procedure to get this fit is described in the document *MJSANL_v_02* in Example 7. John Richardson's heliosheath fits are available at *Voyager_PLS_v_02/v2/daily_hourly_fine/fine/after_shock.*

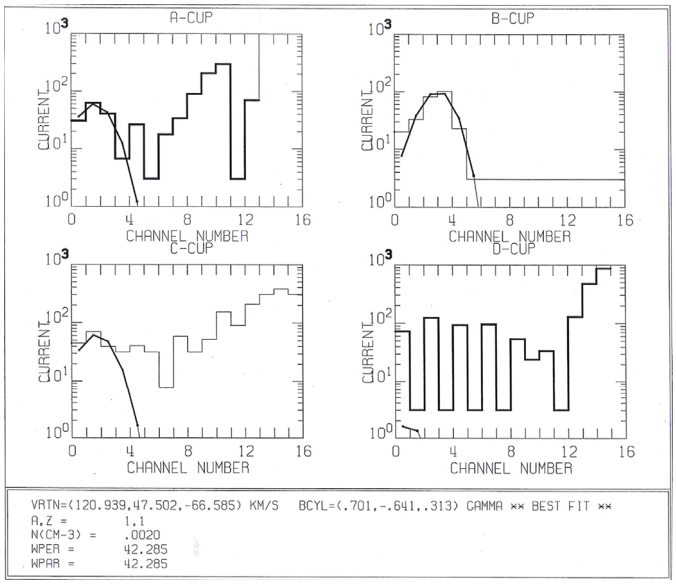

Figure 3.2-2: Heliosheath L Mode Spectra on 2007 day 267 1916 26 136

3.2.3 Fitting a Bi-Maxwellian to Voyager Spectra Assuming Unit Response

In addition to the model-independent moments calculation described above, we also frequently want to find the best fit of a bi-Maxwellian to Voyager spectra. First, we consider fitting a single Maxwellian to one sensor assuming that the sensor response is unity at all angles. We assume the form of our reduced distribution function F is (see 3.1.2.4)

$$F(\mathrm{v}_n) = \int_{-\infty}^{\infty}\int_{-\infty}^{\infty} d\mathrm{v}_{t1} d\mathrm{v}_{t2} f\left(\mathrm{v}_n, \mathrm{v}_{t1}, \mathrm{v}_{t2}\right) = \frac{n}{\sqrt{\pi} w_n} e^{-(\mathrm{v}_n - V_n)^2 / w_n^2} \qquad (3.2.3.1)$$

This gives a density n of

$$n = \int_{-\infty}^{\infty} F(\mathrm{v}_n)\, d\mathrm{v}_n = \int_{-\infty}^{\infty} \frac{n}{\sqrt{\pi} w_n} e^{-(\mathrm{v}_n - V_n)^2 / w_n^2}\, d\mathrm{v}_n = \frac{n}{\sqrt{\pi}} \int_{-\infty}^{\infty} e^{-x^2}\, dx = n \qquad (3.2.3.2)$$

and a thermal speed w_n of

$$w_n^2 = 2\int \left(\mathrm{v}_n - \mathrm{V}_n\right)^2 F(\mathrm{v}_n)\, d\mathrm{v}_n / n = 2\int \left(\mathrm{v}_n - \mathrm{V}_n\right)^2 \frac{n}{\sqrt{\pi} w_n} e^{-(\mathrm{v}_n - V_n)^2 / w_n^2}\, d\mathrm{v}_n \qquad (3.2.3.3)$$

$$w_n^2 = \frac{2}{w_n} \frac{n}{\sqrt{\pi}} w_n^3 \int x^2 e^{-x^2}\, dx = w_n^2 \qquad (3.2.3.4)$$

If we now ask what the current in each channel is when we integrate from the lower velocity window to the upper velocity window of the nth channel, it is given by

$$I_k = q_{proton} A \int_{\mathrm{v}_k}^{\mathrm{v}_{k+1}} d\mathrm{v}_n \mathrm{v}_n \int_{-\infty}^{\infty}\int_{-\infty}^{\infty} d\mathrm{v}_{t1} d\mathrm{v}_{t2} f(\mathbf{v}) = q A_{eff} \int_{\mathrm{v}_k}^{\mathrm{v}_{k+1}} d\mathrm{v}_n \mathrm{v}_n F(\mathrm{v}_n) \qquad (3.2.3.5)$$

$$I_k = q A_{eff} \int_{\mathrm{v}_k}^{\mathrm{v}_{k+1}} d\mathrm{v}_n \mathrm{v}_n \frac{n}{\sqrt{\pi} w_n} e^{-(\mathrm{v}_n - V_n)^2 / w_n^2} = q A_{eff} \frac{n}{\sqrt{\pi} w_n} \int_{\mathrm{v}_k}^{\mathrm{v}_{k+1}} d\mathrm{v}_n \mathrm{v}_n e^{-(\mathrm{v}_n - V_n)^2 / w_n^2} \qquad (3.2.3.6)$$

The above function can be integrated. If we define the *erf* function by

$$erf(z) = \frac{2}{\sqrt{\pi}} \int_0^z e^{-t^2} dt \qquad (3.2.3.7)$$

then we can express the current as

$$I_k = q A_{eff} \frac{n}{2 w_n} \left\{ -\frac{1}{\sqrt{\pi}} e^{-\xi^2} \Big|_{(\mathrm{v}_k - V_n)/w_n}^{(\mathrm{v}_{k+1} - V_n)/w_n} + \left(erf\left((v_{k+1} - V_n) / w_n \right) - erf\left((v_k - V_n) / w_n \right) \right) \right\} \qquad (3.2.3.8)$$

For some purposes, assuming narrow energy windows, we have the approximation:

$$F(\mathrm{v}_n)\Big|_{\mathrm{v}_n = \overline{\mathrm{v}}_k} = I_k / \left[q_{proton} A_{eff} \Delta \mathrm{v}_k \overline{\mathrm{v}}_k \right] = \frac{n}{\sqrt{\pi} w_n} e^{-(\mathrm{v}_k - V_n)^2 / w_n^2} \qquad (3.2.3.9)$$

However, when fitting, we use the full expression involving the *erf* function. The above expression (3.2.3.8) is evaluated in the routine *xcurnt.f* in *software_v_01/mjsanl/code*.

3.2.4 Non-Linear Least Squares Fitting

To find an optimal fit to a Maxwellian to our measurements, we use a non-linear least squares algorythim based on the approach in Chapter 8 of Bevington P. R. and Robinson D. K., *Data Reduction and Error Analysis for the Physical Sciences*, Third Edition, McGraw Hill. A *pdf* copy of this text can be found in *documentation/general/Bevington.pdf* (see Section 1.4.1.1 above). We find the optimal

value of our fitting parameters $\{a_j\}_{j=1}^{m}$ by chosing them to minimize the function χ^2 simultaneously with respect to each parameter:

$$\chi^2 = \sum_i \left\{ \frac{1}{\sigma_i^2} [y_i - y(x_i)]^2 \right\} \tag{3.2.4.1}$$

$$\frac{\partial \chi^2}{\partial a_j} = \frac{\partial}{\partial a_j} \left\{ \sum_i \left\{ \frac{1}{\sigma_i^2} [y_i - y(x_i)]^2 \right\} \right\} = -2 \sum_i \left\{ \frac{1}{\sigma_i^2} [y_i - y(x_i)] \frac{\partial y(x_i)}{\partial a_j} \right\} = 0 \tag{3.2.4.2}$$

This is *m* coupled equation for the *m* parameters $\{a_j\}_{j=1}^{m}$. To search for a best fit, we expand χ^2 to second order in the parameters about a local minimum χ_0^2 where $a_j = a_j'$. If we define $\delta a_j = a_j - a_j'$, then

$$\frac{\partial \chi^2}{\partial (\delta a_k)} = \frac{\partial \chi_o^2}{\partial a_k} + \left\{ \sum_{j=1}^{m} \frac{\partial^2 \chi_o^2}{\partial a_k \partial a_j} \delta a_i \right\} = 0 \tag{3.2.4.3}$$

$$\beta_k - \sum_{j=1}^{m} \delta a_j \alpha_{jk} = 0 \tag{3.2.4.4}$$

$$\beta_k = -\frac{1}{2} \frac{\partial \chi_o^2}{\partial a_k} \qquad \alpha_{jk} = \frac{1}{2} \frac{\partial^2 \chi_o^2}{\partial a_k \partial a_j} \tag{3.2.4.5}$$

In matrix form, this is $\boldsymbol{\beta} = \boldsymbol{\delta a \alpha}$ and if $\boldsymbol{\varepsilon} = \boldsymbol{\alpha}^{-1}$, then

$$\boldsymbol{\delta a} = \boldsymbol{\varepsilon \beta} \tag{3.2.4.6}$$

A non-linear fit to the spectrum at 1977 304 4 59 12 412, using the unit response expression in (3.2.3.8), is shown below.

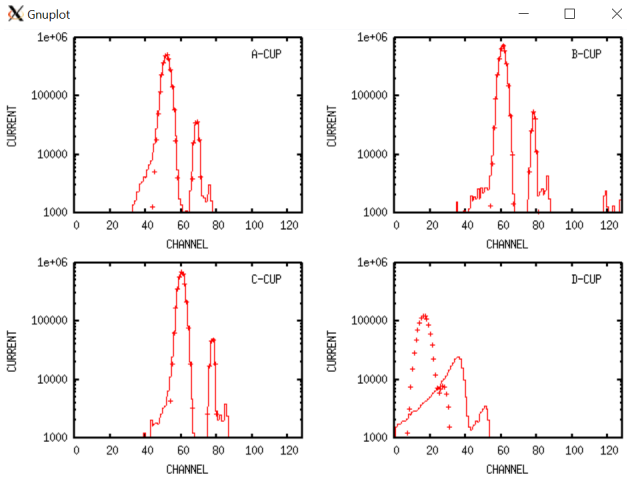

The procedure to get this fit is described in the document *MJSANL_v_02* in Example 4.

3.3 The Measurement Sequence and *M* Start Words

The four measurement modes are the *L* mode (low energy- resolution ions), *M* mode (high energy- resolution ions), *E1* (low energy electron mode, and *E2* (high energy electron mode). They are measured in the time sequence *E1, L, E2, M*. It may take two measurement sequences to get a full M mode, as not all 128 of the energy-per-charge channels of an *M* mode can be returned in one sequence for a given telemetry mode. We return the lower portion of the full 128 *M* mode channels in the first measurement sequence, and then the upper portion of the full 128 *M* mode channels in the second. These subsequent channels may overlap with the channels in the initial scan.

The channel at which a given *M* mode starts is given in the data stream by the *M* start word. If one wants to know the *M* start word for a given *M* mode, the easiest way to do that is to look at a *vgr* file (see Section 7.3 below). As an example, I read a *vgr* file in the directory *software_v_01/telemetry_mstart* as described in Example 3 of *The Voyager PLS Utility Software* (see Section 1.4.2 above). A part of the *output_no_dn* file in that directory is as follows:

```
GS-3  1 1979   94    1    5   43  584  2  2  EFEF0000
GS-3 57 1979   94    1    7   19  584  2  2  EFEF0000
GS-3  1 1979   94    1    8   55  584  2  2  EFEF0000
GS-3 57 1979   94    1   10   31  584  2  2  EFEF0000
GS-3  1 1979   94    1   12    7  584  2  2  EFEF0000
GS-3 57 1979   94    1   13   43  584  2  2  EFEF0000
```

We are in a *GS-3* telemetry mode and the *M* start word is toggling between 1 and 57. When the *M* start word is 1, we get 72 new values for channels 1-72. When the *M* start word is 57, we get 72 new values for channels 57-128. We are sending back 72 new measurements every cycle of the M mode, alternating between 1-72 and 57-128. Note there is an overlap in channels.

Our analysis is on the full set of 128 channels for a given M mode time, even though that consists of current data and data from the previous measurement. Occasionally for

reasons I do not understand, our analysis chokes on this alternation, and we see analyzed data that looks like the intervals below.

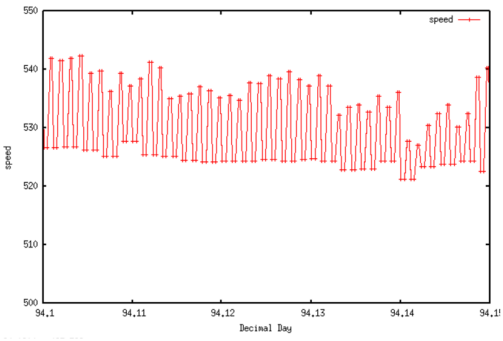

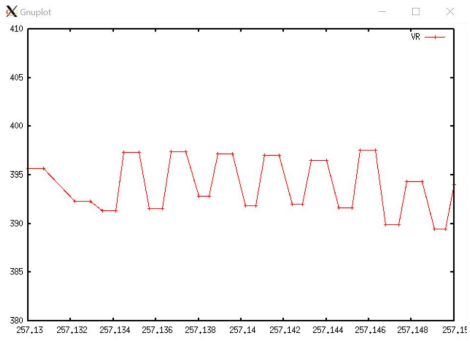

If you see behaviour like this the first thing to do is use *software_v_01/telemetry_mstart* to look at what the *dn* values are from one measurement to the next, to determine where the analysis is flawed. If you can see one *M* start word is consistently giving the incorrect anaysis, you can just chose not to return that measurement based on the value of the *M* start word, although this will halve your time resolution.

This simple *E1, L, E2, M* measurement sequence was drastically altered for the encounters at Uranus and Neptune. See *VoyMemo_202_Neptune_Data*, Table 1, and *VoyMemo_203_Uranus_Data*, Table 1, for a detailed explanation.

3.4 The Status Word

The status word is an 8-bit (one byte) word that indicates the measurement mode of the instrument (*L* mode, *M* mode, low energy electron mode *E1*, and high energy electron mode *E2*), the gain of the instrument, and the calibration mode of the instrument. For example, a status word of *2F* means that we are in the L mode and *IGAN* = 1 and *ICAP* = 0 and the instrument is taking plasma data with the modulator on. Typically, the status word is stored in a full word (four bytes), with the first byte the current status word, the second byte the last good status word previously, and the third and fourth bytes zeroed, for example, *2F2F0000* in hex representation. Sometime, the status word is stored in an INTEGER*2 (two bytes), with the first byte the current status word, the second byte the last good status word previously, for example *2F2F* in hex representation.

Warning: I have converted the data from *Solaris*, which is a big-endian operating system, where the most-significant byte is stored last, to *CentOS*, which is a little-endian operating system where the most-significant byte is stored first. When you are trying to decode a status word using a routine like *l1x* in Section 4.6 below, you must make sure the byte you are giving *l1x* is the appropriate byte, because sometimes you will find it stored in the first byte and sometimes in the last byte of the status word, because of the big/little endian problem.

3.4.1 Bits 1 and 2 of status word code L, E1, E2, M

Table 3.2 shows how the upper two bits of the status word encodes the measurement mode of the instrument.

Mode	Bits 1 and 2
L	(0,0)
E1	(0,1)
E2	(1,0)
M	(1,1)

Table 3-2: Bits 1 and 2 Code L, E1, E2, and M

3.4.2 Bits 3 and 4 of status word code IGAIN and ICAP

(IGAN,ICAP)	Bits 3 and 4
(0,0)	(0,0)
(0,1)	(0,1)
(1,0)	(1,0)
(1,1)	(1,1)

Table 3-3: Bits 3 and 4 Code IGAIN and ICAP

If *IGAN* = 0 the gain *G* is 2.0, if *IGAN* = 1 the gain *G* is 20.0; if *ICAP* = 0 the capacitance *C* is 0.15, and if *ICAP* = 1 the capacitance *C* is 1.15.

3.4.3 Values of bits 1-4 of status word in hexadecimal

We show in this table the values of bits 1-4 in hexadecimal.

			IGAN	ICAP	STATUS	
L	0	0	0	0	0	**0**
L	0	0	0	1	1	**1**
L	0	0	1	0	2	**2**
L	0	0	1	1	3	**3**
E1	0	1	0	0	4	**4**
E1	0	1	0	1	5	**5**
E1	0	1	1	0	6	**6**
E1	0	1	1	1	7	**7**
E2	1	0	0	0	8	**8**
E2	1	0	0	1	9	**9**
E2	1	0	1	0	10	**A**
E2	1	0	1	1	11	**B**
M	1	1	0	0	12	**C**
M	1	1	0	1	13	**D**
M	1	1	1	0	14	**E**

M	1	1	1	1	15	F

Table 3-4: Valid Values of Bits 1-4 of Status Word

3.4.4 Bits 5 through 8 of status word code calibration modes

Calibration Mode	Bits 5-8	Hex Value	Integer Value
DC Return Modulator Off	(0,0,0,0)	0	0
Modulator Calibration	(0,1,1,1)	7	7
Internal Current Calibration	(1,0,1,0)	A	10
DC Return Modulator On	(1,1,0,1)	D	13
Plasma Data Modulator Off	(1,1,1,0)	E	14
Plasma Data Modulator On	(1,1,1,1)	F	15

Table 3-5: Bits 5-8 and Calibration Modes

3.4.5 Code for Status Word Decoding

Suppose we are giving the status word *kstat* as an INTEGER*2, for example *2F2F*. We decode the status word with the following code:

```
      integer icg,l1x
      integer*2 kstat
      icg = l1x(kstat)
      ityp = mod(icg,16)
      ipls = icg/16
      icap = mod(ipls,2)
      igain = mod(ipls/2,2)
      imode = ipls/4
      if(imode .eq.  0) jtlmod =1
      if(imode .eq. 3) jtlmod = 2
      if(imode .eq. 2) jtlmod = 4
      if(imode .eq. 1) jtlmod = 3
```

where the function l1x.f is given by

```
      function l1x(a)
      character*1 a, b(4)
      integer l1x, c
      equivalence (c,b(1))
      data c /0/
      c    = 0
      b(4) = a
      l1x  = c
      return
```

```
      end
```

Here is what this code does. The function *l1x* will take the first byte of *the integer*2 kstat* and put it in the last of four bytes of the *integer icg* (note the argument of *l1x* should be a *character*1*, one byte, but when operating on an *integer*2* variable, *l1x* will take the first byte of the *integer*2* as the input argument). The remaining code determines *ICAP* and *IGAIN* as well as *JTLMOD* (1 for L, 2 for M, 3 for E1, and 4 for E2) from that status word. For the status word *2F2F*, this gives bits 5 through 8 of the status word *ITYP = 15*, or plasma mod on (see Table 3-4 above), with *ICAP = 0, IGAIN* = 1, and *JTLMOD = 1* (an L mode).

Warning: I have converted the data from *Solaris*, which is a big-endian operating system, where the most-significant byte is stored last, to *CentOS*, which is a little-endian operating system, where the most-significant byte is stored first. When you are trying to decode a status word using a routine like *l1x*, you must make sure the byte you are giving *l1x* is the appropriate byte, because sometimes you will find it stored in the first byte and sometime in the last byte of the status word, because of the big/little endian problem. Typically, I will write code like the following to make sure I am taking the right byte out of a status word *lstat*:

```
      character*1 kstat(4),kstat1(4)
      integer lstat,llstat,lllstat
      equivalence (llstat,kstat(1))
      equivalence (lllstat,kstat1(1))
      llstat = lstat
      kstat1(1)=kstat(4)
      kstat1(2)=kstat(3)
      kstat1(3)=kstat(2)
      kstat1(4)=kstat(1)
     write(6,44)  llstat,kstat
     write(6,44)  lllstat,kstat1
 44  format(5z10)
      icg = l1x(lllstat)
c  OR
      icg = l1x(llstat)
c     depending on the output above
```

3.5 DN (digital numbers) and EU (engineering units)

3.5.1 Determining the Threshold

The threshold value T for a given gain G and capacitance C and integration time Δt is given by

$$T = V0 * \frac{C}{G\Delta t} \qquad (3.5.1.1)$$

where $V0$ is 453 for Voyager 1 and 372 for Voyager 2. The values of C and G are determined from the status word and the integration time is specified independent of the

status word on the EDR. Table 3-6 gives the range of threshold values possible for Voyager 1 and 2:

Capacitance (ICAP)	Gain (IGAN)	Integration Time (JCLK)	V1 Threshold	V2 Threshold
0.15 (0)	2 (0)	0.03 (1)	1132.5	930.0
1.15 (1)	2 (0)	0.03 (1)	8682.5	7130.0
0.15 (0)	20 (1)	0.03 (1)	113.3	93.0
1.15 (1)	20 (1)	0.03 (1)	868.3	713.0
0.15 (0)	2 (0)	0.21 (2)	161.8	132.9
1.15 (1)	2 (0)	0.21 (2)	1240.4	1018.6
0.15 (0)	20 (1)	0.21 (2)	16.2	13.3
1.15 (1)	20 (1)	0.21 (2)	124.0	101.9
0.15 (0)	2 (0)	0.93 (3)	36.5	30.0
1.15 (1)	2 (0)	0.93 (3)	280.1	230.0
0.15 (0)	20 (1)	0.93 (3)	3.7	3.0
1.15 (1)	20 (1)	0.93 (3)	28.0	23.0

Table 3-6: Thresholds for Gains, Capacitances and Integration Times Voyager 2

3.5.2 Formula for Conversion DN to EU

Given a DN value from 0 to 255, and the threshold current *T* calculated above, the EU is given by (in femtoamps)

$$EU = \tfrac{1}{2} T * (10^{DN/64} + 10^{(DN+1)/64})$$

3.6 Time Interval between Measurements

3.6.1 Typical Intervals

The longest interval between successive measurements in say the *M* mode is 192 seconds. Other time intervals possible are 96 seconds, 48 seconds, and 12 seconds. We have four months of data on each spacecraft at the 12 second rate (see below).

3.6.2 12 Second Measurements

The is a period of about 4 months on both spacecraft where data was taken at 12 second intervals:

V1 12 sec period 1977 313 23 39 53 428 to 1978 50 22 41 8 688
V2 12 sec period 1977 306 22 9 13 72 to 1978 61 16 37 57 292

This spans the radial distance from 1.324 AU to 2.4 AU for Voyager 1, and for Voyager 2 from 1.34 AU to 2.45 AU.

To achieve this rapidity, measurements during this period were only in the *M* mode cups *A*, *B*, and *C* and in *E1*. There were no *E2* or *L* mode measurements, or any measurements in the *D* cup. There was no alternation of *M* start words; all measurements were from channel 33 to 128.

4 Code Snippets Data Analysis

The code snippets below are from files located in

Voyager_PLS_v_02/software_v_01/historic_libraries/vgr_src_vgr

4.1 Voyager constants: *plsbeg.f*

Among many other things this subroutine sets the values of the constants used in the DN (digital numbers) to EU (Engineering Units, femtoamps) and in the moments calculation.

```
DATA CLOCK/0.03,0.21,0.93/,CAP/0.15,1.15/,GAIN/2.0,20.0/,V0/372.0/
IF ( II.EQ.1 ) V0 = 453.
DATA    NK  /3*9.4419e-4,1.1097e-3,3*9.4419e-4,1.1097e-3/
DATA    SK  /3*9.633E-4,9.179E-4,3*9.633E-4,9.179E-4/
DATA    WK  /3*9.633E-4,9.179E-4,3*9.633E-4,9.179E-4/
DATA    QK  /3*9.633E-4,9.179E-4,3*9.633E-4,9.179E-4/
```

4.2 Converting Digital Number (DN) Values to Currents: kntcur.f

This routine converts DN values to current in femtoamps.

```
C
C   SET UP TABLE FOR DN TO EU CONVERSION
      IADSF =1
      ITYP=MOD(KSTAT/4,4)
C DOESN'T HANDLE HV MONITOR
      IF  (ITYP .EQ. 1)  GO TO 100
      IF(ITYP.EQ.1.OR.
     *  (ITYP.EQ.2.AND.(JTLMOD.EQ.1.OR.ITLMOD.EQ.4))) IADSF=4
      ICPGN=MOD(KSTAT/16,4)
C   CHECK TO SEE IF TABLE HAS ALREADY BEEN SET UP
      IF(ICPGN.EQ.LCPGN.AND.IADSF.EQ.LADSF.AND.JCLK.EQ.LCLK) GO TO 10
      ICAP = MOD(ICPGN/1,2)
      IGAN= ICPGN/2
      FACT = CAP(ICAP+1)/GAIN(IGAN+1)/CLOCK(JCLK)*V0
      NMAX = 256*IADSF
      xxx = 1D0/NMAX
      xxzeta = 1D4**xxx
      xxx = FACT
      NMAX = NMAX+1
```

```
      DO 1 I=1,NMAX
      TABL(I) = xxx
      X0 = SNGL(xxx)
      xxx = xxx*xxzeta
      TABL(I) = 0.5*(X0 + SNGL(xxx))
1     CONTINUE
```

4.3 Generating Voltages and Speeds for Energy Channels: step.f

This code generates the voltages and velocities for the energy channels

```
      SUBROUTINE STEP(NUMCHN)
      IMPLICIT INTEGER*2(I-N)
      COMMON/VSTEP/VLIM(129,2),VAVE(129,2),VDIF(129,2)
      DIMENSION NUMCHN(2),RK(2)
      DATA VLT,DCBIAS/60.,50./
      DATA RK/1.33352,1.03663/
      DATA RT2EM/1.38418E+4/
C
C   SET UP VELOCITY LIMITS FOR L(M=1) AND M(M=2) MODES
C   VELOCITIES ARE CALCULATED IN KM/SEC
C   RT2EM IS SQRT OF CHARGE TO MASS RATIO OF PROTON TIMES TWO
C
      DO 20 M=1,2
      NLIM=NUMCHN(M)+1
      FACTE = RK(M)
      DO 30 L=1,NLIM
      VLIM(L,M)=RT2EM*SQRT(VLT*FACTE**(L-1)-DCBIAS)/1000.
      IF(L.EQ.1) GO TO 30
      VDIF(L-1,M)=VLIM(L,M)-VLIM(L-1,M)
      VAVE(L-1,M)=(VLIM(L,M)+VLIM(L-1,M))/2.
   30 CONTINUE
   20 CONTINUE
      RETURN
      END
```

4.4 Calculating Plasma Moments: *moment.f*

This code is called from *pranal.f* (see Section 4.5 below) to generate the plasma moments in a given cup. The constants FM1, F0, F1, F2 encode the cup areas and the electron charge in the appropriate units, and are given by the values of NK, SK, WK, QK as set in the subroutine *plsbeg.f* (see above). *R* is the current matrix in femtoamps in the cup. *XCRIT* is the current value below which we do not do the sum.

```
      SUBROUTINE
MOMENT(L1,L2,V,R,RMM1,RM0,RM1,RM2,FM1,F0,F1,F2,XCRIT,
     *  IQUALY)
      IMPLICIT INTEGER*2 (I-N)
C       DATE   JAN  9 1978
      DIMENSION V(128),R(512),RV(128)
C
C   RMM1 IS DENSITY (CM-3)
C   RM0 IS VEL (KM/SEC)
C   RM1 IS THERMAL SPEED ((KM/SEC)**2)
C   RM2 IS THIRD MOMENT DIVIDED BY DENSITY ((KM/SEC)**3)
C
      IQUALY=0
      RMM1=0.
      RM0=0.
      RM1=0.
      RM2=0.
      DO 10 L=L1,L2
      IF(R(L).LE.XCRIT) GO TO 10
      IQUALY = IQUALY+ 1
      RV(L)=R(L)/V(L)
      RMM1=RMM1+RV(L)
      RM0 = RM0 + R(L)
   10  CONTINUE
      IF(RMM1.NE.0.) GO TO 30
      IF (IQUALY.EQ.0) RETURN
      PRINT 2649,L1,L2,RMM1,RM0,RM1,RM2,FM1,F0,F1,F2,RV
       IQUALY = -IQUALY
      RETURN
30    RMM1=FM1*RMM1
      RM0= F0*RM0/RMM1
      DO 20 L=L1,L2
      IF(R(L).LE.XCRIT) GO TO 20
      DEL= V(L)-RM0
      PROD=RV(L)*(DEL**2)
      RM1=RM1+PROD
      RM2 = RM2 + PROD*DEL
   20   CONTINUE
      RM1= 2.*F1*RM1/RMM1
      RM2= F2*RM2/RMM1
      IF (RM1.GE.0) RETURN
      PRINT 2649,L1,L2,RMM1,RM0,RM1,RM2,FM1,F0,F1,F2,RV
      RM1 = -RM1
       IQUALY = -IQUALY
      RETURN
 2649 FORMAT (' MOMENT ERROR',2I4,8G12.3/(1X,10G12.4))
```

```
      END
```

4.5 Moment Analysis of Proton Data: *pranal.f*

```
   DO 10 K=1,NCUP
      JX = (K-1)*NE+1
      IP=IPK(K)
      IF(IP.EQ.0.AND.K.EQ.4) GO TO 10
C
      IF(K.EQ.4) GO TO 5001
      IF(IP.EQ.0) RETURN
C
C
 5001 J1=MAX0((IP-IPQ(K,MD))*1,1)
      J2=MIN0((IP+IPR(K,MD))*1,NE*1)
      ANS(K)=A(JX+IP-1)
      ANS(K+4)=IP
      JN = 12+K
      JV = 16+K
      JW = 26+K
      JQ = 35+K
c          let us not look outside gap of more that n1 "0" channels
           n1 = 2
           n1 = 1
           ipt = ip
           call przero( n1, ipt, a(jx), rmark, j1, j2)
           j1a(k,1) = j1
           j2a(k,1) = j2
      IF(MD.EQ.1)
     1 CALL MOMENT(J1,J2,VJNL,A(JX),ANS(JN),ANS(JV),ANS(JW),ANS(JQ),
     2 NK(K,1),SK(K,1),WK(K,1),QK(K,1),XCRIT,IQUALY)
      IF(MD.EQ.2)
     1 CALL MOMENT(J1,J2,VJNM,A(JX),ANS(JN),ANS(JV),ANS(JW),ANS(JQ),
     2 NK(K,2),SK(K,2),WK(K,2),QK(K,2),XCRIT,IQUALY)
      ANS(K+8)=IQUALY
c     IF(IQUALY.LT.3.AND.K.NE.4)LQUAL=.TRUE.
c
c Criterion changed due to COLD solar wind at large
c heliocentric distences; SW is many times confined to only
c 2 M-mode channels
c
c Change made by rlm 3/13/89
c Changed by gsg jr 4/26/89 to voyager memo # 176
      IF(IQUALY.LT.iqualm.AND.K.NE.4)LQUAL=.TRUE.
   10 CONTINUE
```

4.6 Manipulating bits in the status word: *l1x*

This function routine takes a single byte and puts it in the last byte of the four bytes of a full word, zeroing out the first, second, and third bytes. Then using mod operations one can recover the bits in the status word. If the variable "*a*" in the calling argument is a full four-byte word, this routine will put the first byte of that word into the last byte of the four-byte word returned. If the variable "a" in the calling argument is an integer*2, this routine will put the first byte of that word into the last byte of the four-byte word returned.

```
function l1x(a)
character*1 a, b(4)
integer l1x, c
equivalence (c,b(1))
data c /0/
c    = 0
b(4) = a
l1x  = c
return
end
```

Warning: See the cautions in Section 3.4.5 above.

5 Trajectory and Pointing

5.1 Coordinate Systems

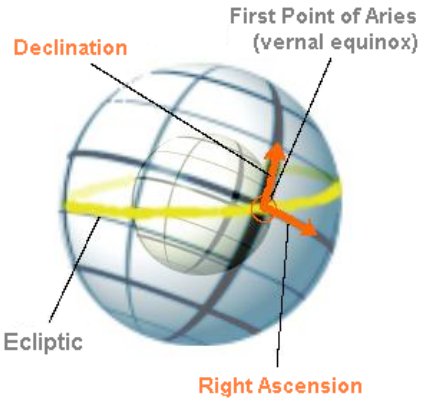

5.1.1 Earth Equatorial to Ecliptic ECL50

The right ascension α and declination δ of a star in earth equatorial coordinates can be used to compute the ECL50 XYZ components of the direction to the star as follows. First calculate the XYZ coordinates in earth equatorial coordinates using the following equation

$$\mathbf{X}_{\text{equatorial}} = \begin{pmatrix} \cos\delta\cos\alpha \\ \cos\delta\sin\alpha \\ \sin\delta \end{pmatrix} \qquad (5.1.1.1)$$

Then rotate this vector about the X-axis by φ = 23.445789 degrees, the tilt of the earth's spin axis from the normal to the plane of its orbit, to get the coordinates of the vector in ECL50.

$$\mathbf{X}_{\text{ECL50}} = \begin{pmatrix} 1 & 0 & 0 \\ 0 & \cos\varphi & \sin\varphi \\ 0 & -\sin\varphi & \cos\varphi \end{pmatrix} \mathbf{X}_{\text{equatorial}} \tag{5.1.1.2}$$

5.1.2 ECL50

The ECL50 coordinate system is based on the ecliptic plane, that is, the plane of the orbit of the earth about the sun. The x-axis of this system is defined by the intersection of the plane of the earth's orbit with the plane of the earth's rotational equator, with zero longitude being defined in terms of the ascending node.

5.1.3 RTN Heliographic

RTN Heliographic coordinates are based on the rotational equator of the sun (which defines the solar equatorial plane). The normal to that plane is tilted at an angle of θ_s =7.25 degrees from the normal to the ecliptic. The intersection of the plane of the solar equator and of the ecliptic occurs defines the x axis of the RTN system, with the longitude of the ascending note (the x axis of RTN) at an angle of ϕ_s =75.07 degrees as measured in ECL50 coordinates.

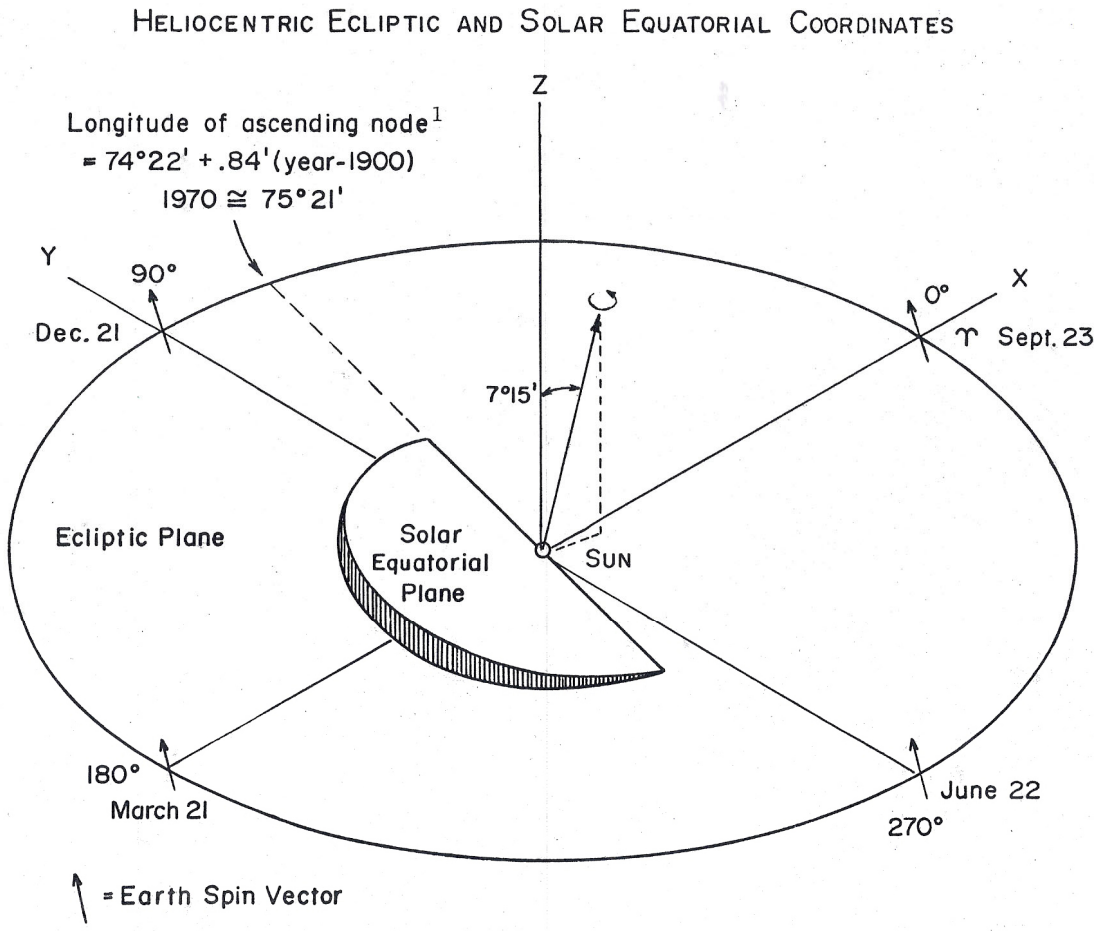

Figure 5.1-1: Ecliptic and Solar Equatorial Coordinates

To rotate from ECL50 to RTN coordinates, we first rotate in the *xy* ECL50 plane to get to the RTN x-axis and then rotate about the x-axis to tilt the z-axis over to the appropriate orientation. That is, if $\mathbf{X}_{ECL50}$ is a Cartesian coordinate vector in ECL50, then its Cartesian coordinate vector in RTN, $\mathbf{X}_{RTN}$, is given by

$$\mathbf{X}_{RTN} = \begin{pmatrix} 1 & 0 & 0 \\ 0 & \cos\theta_s & \sin\theta_s \\ 0 & -\sin\theta_s & \cos\theta_s \end{pmatrix} \begin{pmatrix} \cos\phi_s & \sin\phi_s & 0 \\ -\sin\phi_s & \cos\phi_s & 0 \\ 0 & 0 & 1 \end{pmatrix} \mathbf{X}_{ECL50} \tag{5.1.3.1}$$

or

$$\mathbf{X}_{RTN} = \begin{pmatrix} \cos\phi_s & \sin\phi_s & 0 \\ -\cos\theta_s \sin\phi_s & \cos\theta_s \cos\phi_s & \sin\theta_s \\ \sin\theta_s \sin\phi_s & -\sin\theta_s \cos\phi_s & \cos\theta_s \end{pmatrix} \mathbf{X}_{ECL50} \tag{5.1.3.2}$$

We can invert this
to give

$$\mathbf{X}_{\mathbf{ECL50}} = \begin{pmatrix} \cos\phi_s & -\sin\phi_s & 0 \\ \sin\phi_s & \cos\phi_s & 0 \\ 0 & 0 & 1 \end{pmatrix} \begin{pmatrix} 1 & 0 & 0 \\ 0 & \cos\theta_s & -\sin\theta_s \\ 0 & \sin\theta_s & \cos\theta_s \end{pmatrix} \mathbf{X}_{\mathbf{RTN}} \tag{5.1.3.3}$$

or

$$\mathbf{X}_{RTN} = \begin{pmatrix} \cos\phi_s & -\cos\theta_s \sin\phi_s & \sin\theta_s \sin\phi_s \\ \sin\phi_s & \cos\theta_s \cos\phi_s & -\sin\theta_s \cos\phi_s \\ 0 & \sin\theta_s & \cos\theta_s \end{pmatrix} \mathbf{X}_{ECL50} \tag{5.1.3.4}$$

5.1.4 IHC Interstellar Heliospheric Coordinates

Although I give this definition here, to my knowledge this coordinate system has never been used in any analysis. We now define *IHC* coordinates as a coordinate system whose *z-axis* lies in the direction opposite to the interstellar wind direction. This is the direction to the inflow of neutrals into the solar systems, and we use the directions given by Lallement et al. (1990). These authors give the direction to the incoming neutrals of ecliptic longitude λ of 252 degrees and ecliptic latitude β of 7 degrees, a speed of 20 km/s, and a temperature *T* of 8000 K. The components of this vector in *ECL50* are

$$Z_{\mathrm{IHC}}^{\mathrm{ECL50}} = \begin{pmatrix} \cos\delta\cos\lambda \\ \cos\delta\sin\lambda \\ \sin\delta \end{pmatrix} = \begin{pmatrix} \text{-}0.306714 \\ \text{-}0.943967 \\ 0.121869 \end{pmatrix} \tag{5.1.4.1}$$

If we use the transformation from *ECL50* to *RTN* given above this gives us

$$Z_{\mathrm{IHC}}^{\mathrm{RTN}} = \begin{pmatrix} \text{-}0.991122 \\ 0.068112 \\ 0.1141867 \end{pmatrix} \tag{5.1.4.2}$$

Note that this vector lies almost in the solar equatorial plane.

Now we define the *x-axis* and *y-axis* of our *IHC* coordinates such that

$$\mathrm{X}_{\mathrm{IHC}} = \frac{\mathbf{Z}_{\mathrm{RTN}} \times \mathbf{Z}_{\mathrm{IHC}}}{\left|\mathbf{Z}_{\mathrm{RTN}} \times \mathbf{Z}_{\mathrm{IHC}}\right|} \qquad \mathrm{Y}_{\mathrm{IHC}} = \mathbf{Z}_{\mathrm{IHC}} \times \mathbf{X}_{\mathrm{IHC}} \tag{5.1.4.3}$$

which in RTN are given by

$$X_{IHC}^{RTN} = \begin{pmatrix} -0.068560 \\ -0.997647 \\ 0.0 \end{pmatrix} \qquad Y_{IHC}^{RTN} = \begin{pmatrix} 0.113918 \\ -0.007829 \\ 0.993459 \end{pmatrix} \qquad (5.1.4.4)$$

Note that the *z-axis* in *IHC* is almost the negative x-axis in *RTN*, the *x-axis* in IHC is almost the negative y axis in RTN, and that the y-axis in IHC is almost the z-axis in RTN.

5.1.5 Going from Measured Cup Speeds to Velocity in *RTN* or *IHC*

We summarize the procedure for going from a measurement of V_A, V_B, and V_C from the observed data to the velocity vector in RTN or IHC. First, we use equations (2.2.11) through (2.2.13) to find the velocity components in *s/c* coordinates. Then we use the pointing information from the *SEDR*, which gives the *s/c* axes in *ECL50*, to find the velocity components in *ECL50*. Then we must correct for aberration by ***adding*** the *s/c* velocity in *ECL50* coordinates to the velocity vector in *ECL50* we just computed. The *s/c* velocity in *ECL50* is also given in the *SEDR*. Then we have the velocity vector in *ECL50*, and we can transform that vector from *ECL50* to *RTN* or IHC using the transformations given above.

5.2 Lock stars

We show below a table that gives the common lock stars for Voyager, their right ascension and declination, and their *ECL50* coordinates, computed using equations 5.1.1.1 and 5.1.1.2.

Table 5-1: Lock stars and their *ECL50* Coordinates

Lock Star	Declination α	Right Ascension δ	X ECL50	Y ECL50	Z ECL50
CANOPUS	-52.6674	95.7107	-0.060344	0.237243	-0.969574
RIGILKENTAURUS	-60.6243	218.9856	-0.381294	-0.629850	-0.676686
HADAR	-60.133	210.0684	-0.430973	-0.573945	-0.696311
ACRUX	-62.8222	185.9498	-0.454293	-0.397389	-0.797308
SPICA	-10.9012	200.6384	-0.918936	-0.392778	-0.035792
ARCTURUS	19.4253	213.3351	-0.787912	-0.343138	0.511322
MIMOSA	-59.4158	191.1954	-0.499122	-0.433160	-0.750500
MIAPLACIDUS	-69.5101	138.1616	-0.260792	-0.158497	-0.952295
VEGA	38.74	278.81	0.119463	-0.458163	0.880804
FOMALHAUT	-29.89	343.73	0.832263	-0.421122	-0.360548
ALKAID	49.5621	206.3913	-0.581023	0.038322	0.812984
ACHERNAR	-57.4905	23.9654	0.491107	-0.135258	-0.860534
DENEB[1]	45.27	310.325	0.45542	-0.20958	0.86526

[1] From http://www.astro.utoronto.ca/~garrison/oh.html

5.3 Generating Pointing Given the Lock star and $\mathbf{Z}_{s/c}$

If we know the vector $\mathbf{Z}_{s/c}$ and the lock star, we can compute the orientation of the spacecraft axes as follows. Let **S** be the vector in ECL50 of the lock star, and assume we know the spacecraft z-axis in *ECL50* as well (this is the earth spacecraft vector and is usually given in the navigation block of the *SEDR*). We define the two directions

$$\hat{\mathbf{Y}}_S = \frac{\hat{\mathbf{Z}}_{s/c} \times \mathbf{S}}{\left|\hat{\mathbf{Z}}_{s/c} \times \mathbf{S}\right|} \qquad \hat{\mathbf{X}}_S = \hat{\mathbf{Y}}_S \times \hat{\mathbf{Z}}_{s/c} \tag{5.3.1}$$

Given this construction, we can compute the spacecraft **X** and **Y** axes using the equations (refer to Figure 2.1-3)

$$\hat{\mathbf{X}}_{s/c} = \hat{\mathbf{X}}_S \cos 55^\circ + \hat{\mathbf{Y}}_S \sin 55^\circ \tag{5.3.2}$$

$$\hat{\mathbf{Y}}_{s/c} = \hat{\mathbf{Y}}_S \cos 55^\circ - \hat{\mathbf{X}}_S \sin 55^\circ \tag{5.3.3}$$

For example, on the Short *SEDR* file for $2009^{y}\ 1^{d}\ 23^{h}\ 59^{m}\ 59s\ 1^{ms}$, the vector for the spacecraft z-axis in *ECL50* is given as (0.2663, -0.8042, 0.5313). If we assume the lock star is *Vega* and use its *ECL50* components as given in Table 5.1, then we find using the equations above that the predicted spacecraft *X* axes has *ECL50* components of (-0.7024,-0.5394,0.4644) and the predicted spacecraft *Y* axis has components of (-0.6601,0.2495,-0.7086). These are the same as the values given in the pointing block to four significant figures.

5.4 Short *SEDR* File Format for Cruise

This section is based on *VoyMemo_180_Trajectory_Files_Cruise_3_Revisions*. For encounters the format is different from cruise, as documented in *VoyMemo_200_Planetary_SSEDR_Files_v_02* (see Section 5.5 below). A short *SEDR* is a shortened version of a full *SEDR* (*Supplemental Experiment Data Record*). Items 1-62 below are from the *Navigation Block* of the full *SEDR* (containing information about the location of the *S/C*, planets, and so on). Items 63-79 below are from the *Pointing Block* of the full *SEDR* (containing information about the orientation of the *S/C*). The *Cartesian State* of an object is six words long. The first three words contain the location of the object referred to in *ECL50* coordinates; the second three words of the Cartesian State are the velocity components of the object referred to in *ECL50*.

Table 5-2: The format of the Short *SEDR* file*

Word #	Type	Description
1-6	Int*4	SCE UTC year,day,hr,mn,s,ms
7-18	Real*4	Cart. St. of S/C; Earth and Sun centered ECL5O (km,km/s)[2]
19-30	Real*4	See Note[3]
31-36	Real*4	Cart. St. of Earth in Sun centered ECL5O
37-48	Real*4	Cart. St. of Jupiter and Saturn in Sun centered ECL5O
49	Real*4	Range of S/C from Sun (km)
50	Real*4	Earth-Sun-S/C angle
51-62	Real*4	Cart. St. of Uranus and Neptune in Sun centered ECL5O
63-70	Int*4	SCE UTC[4] and FDSC MOD16 and MOD60
71-79	Real*4	Cart. unit vector for S/C X,Y,Z axis in S/C centered ECL5O (Rotation matrix from S/C to ECL5O coordinates)

*These 79 words are preceded and followed by the number of bytes in the file, 4*79=316. This comment is for the binary files on *Solaris*.

The time resolution of the files is 5 days unless a change of at least 1 degree takes place in which case the change is bracketed. All data was written with FORTRAN unformatted write. Note that on the Voyager 2 short *SEDR* files there is a long gap of about 18 days between the following times: 1979 186 18 2 23 220 and 1979 205 0 2 21 984. There are also frequent gaps of length around 5.1 days, and one longer gap around 6 days. If the user is really worried about time coverage, he or she should check the *SEDR* for gaps in coverage around the time of interest.

These binary files on *Solaris* have been converted to *ascii* files, which can be found in *Voyager_PLS_v_02/v2/cruise_ssedr* and *Voyager_PLS_v_02/v2/cruise_ssedr.*

5.5 Short *SEDR* File Format for Encounters

Short SEDR files for encounters are like those for cruise, except the format differs for the various planets, as explained below.

5.5.1 Jupiter

---

[2] The earth centered is first, then sun centered.
[3] For data originating from Launch or Cruise tapes, items 19 - 24 and 25 - 30 are the Cartesian state of the S/C in Jupiter and Saturn centered ECLSO coordinates (km, km/s), respectively. For data originating from Extended Cruise tapes, items 19 - 24 and 25 - 30 are the Cartesian state of the S/C in Uranus and Neptune centered ECLSO coordinates, respectively. When Extended Cruise data are used, items 51 - 62 are set to 0.0.
[4] This time usually differs from the time in 1-6 by less than a sec, but this are in fact different times at which the variables are evaluated.

We have converted all the binary *ssedr* files for Jupiter to two *ascii* files, *ssedr.v1.jup.txt* and *ssedr.v2.jup.txt*, which can be found in the directories *Voyager_PLS_v_02/v1/encounter_ssedr* and *Voyager_PLS_v_02/v2/encounter_ssedr*, respectively. For the details of which binary files have gone into these two files, see *Voyager Memo 200: Planetary SSEDR Files.* The *v1* file covers

Time period: 1979 59 0 0 0 0 to 1979 79 23 45 0 0
Radial distance: 95 Jovian radii in-bound to 263 Jovian radii out-bound

and the *v2* file covers

Time period: 183 10 0 0 0 to 1979 215 23 58 24
Radial distance: 101 Jovian radii in-bound to 285 Jovian radii out-bound

The read routines for these files are:

```
    real nav(27), point(9)
    integer ntn(6), ntp(6)
    read(5,200,end=1000) ntn,nav,ntp,point
200 format(6I5,27E16.8,6I5,9E16.8)
```

where the meaning of the input variables is:

Nav Word #	Description
1-6	Cartesian State of S/C, Jupiter Centered, Jupiter System III, True Prime Meridian and Equator of Date (km, km/s)
7-12	Cartesian State of S/C, Jupiter Centered, Earth Mean Ecliptic and Equinox of 1950 (km, km/s)
13-15	Cartesian Position of Io, Jupiter Centered, Jupiter System III, True Prime Meridian and Equator of Date (km)
16-18	Cartesian Position of Europa, Jupiter Centered, Jupiter System III, True Prime Meridian and Equator of Date (km)
19-21	Cartesian Position of Ganymede, Jupiter Centered, Jupiter System III, True Prime Meridian and Equator of Date (km)
22-24	Cartesian Position of Callisto, Jupiter Centered, Jupiter System III, True Prime Meridian and Equator of Date (km)
25-27	Cartesian Position of Callisto, Jupiter Centered, Earth Mean Ecliptic and Equinox of 1950 (km)

Pointing Word #	Description
1-9	R(1,1),R(2,1),R(3,1),R(1,2),R(2,2),R(3,2), R(1,3),R(2,3),R(3,3) Rotation matrix *from* S/C *to* ECL50

	$\left(\mathbf{X}_{ECL50}\right)^i = \sum_j R_{ij}\left(\mathbf{X}_{S/C}\right)^j$

5.5.2 Saturn

We have converted all the binary *ssedr* files for Saturn to two *ascii* files, *ssedr.v1.sat.txt* and *ssedr.v2.sat.txt*, which can be found at in the directories *Voyager_PLS_v_02/v1/encounter_ssedr* and *Voyager_PLS_v_02/v2/encounter_ssedr*, respectively (see Section 7.3 below). For the details of which binary files have gone into these two files, see *Voyager Memo 200: Planetary SSEDR Files.*

Time period covered: Voyager 1: 1980 316 0 0 34 933 to 319 10 56 35 59
Radial distance: 50 Saturnian radii in-bound to 38 Saturnian radii out-bound

Time period covered: Voyager 2: 1981 236 0 1 35 597 to 1981 239 5 58 23 316
Radial distance: 42 Saturnian radii in-bound to 24 Saturnian radii out-bound

The read routines for these files are (note the differences with Jupiter)

```
    real nav(18), point(9)
    integer ntn(6), ntp(6)
    read(5,200,end=1000) ntn,nav,ntp,point
200 format(6I5,18E16.8,6I5,9E16.8)
```

where the meaning of the input variables is:

Nav Word #	Description
1-6	Cartesian State of S/C, Saturn Centered, Saturn True Prime Meridian and Equator of Date (km,km/s)
7-12	Cartesian State of S/C, Saturn Centered, Earth Mean Ecliptic and Equinox of 1950 (km,km/s)
13-15	Cartesian Position of Titan, Saturn Centered, Earth Mean Ecliptic and Equinox of 1950 (km)
16-18	Not used

The pointing variables are the same as for Jupiter above.

5.5.3 Uranus

We have converted all the binary *ssedr* files for Uranus to one *ascii* file, *ssedr.v1.ura.txt*, which can be found at in the directory *Voyager_PLS_v_02/v2/encounter_ssedr*. For the details of which binary files have gone into this file, see *Voyager Memo 200: Planetary SSEDR Files.*

Time period: 1986 22 2 43 12 214 to 1986 33 13 3 59 123
Radial distance: 130 Uranian radii in-bound to 429 Uranian radii out-bound

The read routines for these files are (note the differences with Saturn)

```
    real nav(27), point(9)
    integer ntn(6), ntp(6)
    read(5,200,end=1000) ntn,nav,ntp,point
200 format(6I5,27E16.8,6I5,9E16.8)
```

where the meaning of the input variables is:

Nav Word #	Description
1-6	Cartesian State of S/C, Uranus Centered, Uranus True Prime Meridian and Equator of Date (km, km/s)
7-12	Cartesian State of S/C, Uranus Centered, Earth Mean Ecliptic and Equinox of 1950 (km, km/s)
13-15	Cartesian Position of Miranda, Uranus Centered, Uranus True Prime Meridian and Equator of Date (km)
16-18	Cartesian Position of Ariel, Uranus Centered, Uranus True Prime Meridian and Equator of Date (km)
19-21	Cartesian Position of Umbriel, Uranus Centered, Uranus True Prime Meridian and Equator of Date (km)
22-24	Cartesian Position of Titania, Uranus Centered, Uranus True Prime Meridian and Equator of Date (km)
25-27	Cartesian Position of Titania, Uranus Centered, Earth Mean Ecliptic and Equinox of 1950 (km)

The pointing variables are the same as for Jupiter above.

5.5.4 Neptune

We have converted all the binary *ssedr* files for Neptune to one *ascii* file, *ssedr.v1.nep.txt*, which can be found at in the directory *Voyager_PLS_v_02/v2/encounter_ssedr*. For the details of which binary files have gone into this file, see *Voyager Memo 200: Planetary SSEDR Files.*

Time period: 1989 236 0 to 1989 238 4
Radial distance: 71 Neptunian radii in-bound to 62 Neptunian radii out-bound

The read routines for these files are (note the differences with Uranus)

```
    real nav(18), point(9)
    integer ntn(6), ntp(6)
    read(5,200,end=1000) ntn,nav,ntp,point
200 format(6I5,18E16.8,6I5,9E16.8)
```

where the meaning of the input variables is:

Nav Word #	Description
1-6	Cartesian State of S/C, Neptune Centered, Neptune True Prime Meridian and Equator of Date (km, km/s)
7-12	Cartesian State of S/C, Neptune Centered, Earth Mean Ecliptic and Equinox of 1950 (km, km/s)
13-15	Cartesian Position of Triton, Neptune Centered, Neptune True Prime Meridian and Equator of Date (km)
16-18	Not used

The pointing variables are the same as for Jupiter above.

6 Code Snippets Trajectory/Pointing Data

6.1 Lock Stars: *refer.f*

The code below is a subroutine *refer.f*, a fortran file in *software_v_01/historic_libraries/vgr_src_sedr.*

```
c ***** used August 1989 at O.I.T. to create SEDR with pointing for
GSFC
C
C 8/15/89
C MODIFIED TO PRODUCE IBM FORMAT TAPE FOR GSFC
C PRODUCTION DURING NEPTUNE ENCOUNTER OB AND FE PHASES.
C USES PREDICT SEDR WITH NAV ONLY AS INPUT.
C
C IF NO POINTING INFO IS PRESENT, SXRED CALLS THIS ROUTINE
C WITH N=1 AND ONLY TWO ARGUMENTS: ISR AND STAR; THE LATTER
C IS TO BE RETURNED TO CALCULATE THE POINTING VIA THE SUBROUTINE
C NOMDIR.
C
C RLM
C
      SUBROUTINE REFER (/N/,STAR,STRNM)
C     N SPECIFIES THE REFERENCE STAR
C
C         1           CANOPUS
C         2    RIGILKENTAURUS
C         3              HADAR
C         4              ACRUX
C         5              SPICA
C         6           ARCTURUS
C         7             MIMOSA
C         8       MIAPLACIDUS
C         9               VEGA
C        10          FOMALHAUT
C        11             ALKAID
C        12           ARCHENAR
C
C     'STAR' CONTAINS THE CARTESIAN COORDINATES OF THE UNIT VECTOR
C     POINTING TO THE REFERENCE STAR IN THE ECL50 SYSTEM
C
C ACCESS TIME OF NAVIGATION BLOCK
```

```
C
      COMMON/NAVBUF/NAV(252)
      DIMENSION STAR(1)
      DIMENSION STRNM(1)
      REAL*4 R(6,12)
      LOGICAL LFIRST
      DATA LFIRST /.TRUE./
      DATA R   /'    ','    ',' CAN','OPUS',-52.6674, 95.7107,
     2          ' RIG','IL K','ENTA','URUS',-60.6243,218.9856,
     3          '    ','    ','   H','ADAR',-60.1330,210.0684,
     4          '    ','    ','   A','CRUX',-62.8222,185.9498,
     5          '    ','    ','   S','PICA',-10.9012,200.6384,
     6          '    ','    ','ARCT','URUS', 19.4253,213.3351,
     7          '    ','    ','  MI','MOSA',-59.4158,191.1954,
     8          '    ',' MIA','PLAC','IDUS',-69.5101,138.1616,
     9          '    ','    ','    ','VEGA', 38.74  ,278.81  ,
     A          '    ','   F','OMAL','HAUT' -29.89  ,343.73  ,
     B          '    ','    ','  AL','KAID', 49.5621,206.3913,
     C          '    ','    ','ACHE','RNAR',-57.4905, 23.9654/
      DATA IT1/77461/
      DATA IT2/1072981/
      DATA IT3/9649103/
C
C ALKAID AND ACHENAR ADDED 8/15/89 FOR NEPTUNE ENCOUNTER;
C COORDINATES ARE DEC AND R.A. FOR JAN. 1, 1980 IN EME50
C (FROM P.III-247 OF JPL 618-116).
      CALL NUMP(NARG)
      EP0=23.445789
      RD=3.141593/180.
C
C LOOP AROUND IF NOT NEPTUNE ENCOUNTER
C
      IF (NAV(1) .NE. 1989) GO TO 10
      N=1
C
C STAY ON CANOPUS IF
C      BEFORE 1989-116/0000:00 OR AFTER 1989-227/2359:59
C
      IF (NAV(2) .LT. 116) GO TO 10
      IF (NAV(2) .GT. 227) GO TO 10
C
C CHANGE TO ALKAID   (N=11) AT 1989-116/2131:01 IT1=  77461.0
C CHANGE TO ACHERNAR (N=12) AT 1989-128/1003:01 IT2=1072981.0
C CHANGE TO CANOPUS  (N=1)  AT 1989-227/1618:23 IT3=9649103.0
C
      IT= (NAV(2)-116)*24 + NAV(3)
      IT=IT*3600+NAV(4)*60+NAV(5)
C
C VARIABLE "IT" IS THE NUMBER OF SECONDS FROM THE
C BEGINNING OF DAY 116 (OF 1989).
C
      IF (IT .LT. IT1) GO TO 10
      IF (IT .GT. IT3) GO TO 10
      IF (LFIRST) PRINT 2673
      LFIRST = .FALSE.
 2673 FORMAT (/,' FIRST USE OF A NON-CANOPUS STAR BY REFER ROUTINE.')
      IF ((IT .GE. IT1) .AND. (IT .LT. IT2)) N=11
```

```
      IF ((IT .GE. IT2) .AND. (IT .LT. IT3)) N=12
C
C CONTINUE EXECUTION AND GENERATE VECTOR STAR
C
   10 CONTINUE
      X=COS(RD*R(5,N))*COS(RD*R(6,N))
      Y=COS(RD*R(5,N))*SIN(RD*R(6,N))
      Z=SIN(RD*R(5,N))
      STAR(1)=X
      STAR(2)=Y*COS(RD*EP0)+Z*SIN(RD*EP0)
      STAR(3)=-Y*SIN(RD*EP0)+Z*COS(RD*EP0)
      IF (NARG .EQ. 2) RETURN
C **  DO 1 I=1,4
C * 1    STRNM(I)=RCHAR(I,N)
      RETURN
      END
```

6.2 Transforming from *ECL50* to *RTN* (solar heliographic): *helio.f*

See *VoyMemo_033_Rotate_from_SC_Coordinates.pdf*. The code below is a subroutine to go from *ECL50* to *RTN*.

```
         subroutine HEEC(xh,xe)
         dimension xh(3),xe(3),r(3,3)
   c  routine to rotate vector in ecl50 to heliograhic
   c  see voyager memo #33
   c  note:  the x axis of heliographic is along the
   c  longitude of the ascending node
         data phis/75.07/, ts/7.25/
         data rd/57.29578/
         data istart/0/
   c  set up rotation matrix first time through
         if(istart.ne.0) go to 10
         istart = 1
         p=phis/rd
         t=ts/rd
         r(1,1)=cos(p)
         r(1,2)=sin(p)
         r(1,3)=0.
         r(2,1)=-sin(p)*cos(t)
         r(2,2)=cos(p)*cos(t)
         r(2,3)=sin(t)
         r(3,1)=sin(p)*sin(t)
         r(3,2)=-cos(p)*sin(t)
         r(3,3)=cos(t)
     10  continue
         do 20 i=1,3
         xh(i)=0.
         do 30 j=1,3
         xh(i)=xh(i)+r(i,j)*xe(j)
     30  continue
     20  continue
         return
         end
```

7 *PLS* Cruise and Encounter Data and Calibrations

7.1 Calibration files

As described in *VoyMemo_197_calibration_files*, I have gone through the mission and gathered calibrations for both Voyager 1 and Voyager 2. For Voyager 1, the calibrations come entirely from the summary files in *Voyager_PLS_v_02/v1/summary*. For Voyager 2, the calibrations come from the summary files in *Voyager_PLS_v_02/v2/summary* until the end of the summaries from Goddard in 1989 and then from the *edr* files in *Voyager_PLS_v_02/v2/edr* from 1990 through 2022. Note that there is a significant gap of time (more than a year) between when the summaries stop and the *edr*'s begin. We do not have calibrations in this gap (we do have plasma data in this period).

For a given year, I have gathered the following kinds of calibrations (below is for 1977 but files exist for each year):

E1-curcal_1977
E2-curcal_1977
L-curcal_1977
M-curcal_1977
E1-curcal_modon_1977
E2-curcal_modon_1977
L-curcal_modon_1977
M-curcal_modon_1977
E1-DCreturn_modon_1977
E2-DCreturn_modon_1977
L-DCreturn_modon_1977
M-DCreturn_modon_1977
E1-modcal_1977
E2-modcal_1977
L-modcal_1977
M-modcal_1977

These files can be found in *Voyager_PLS_v_02/v1/calibrations* and *Voyager_PLS_v_02/v2/calibrations.*

The four different calibrations for each mode are as follows (these correspond to the commands AJ13, AJ10, AJ11, and AJ07):

13	DCreturn_modon
10	curcal
11	curcal_modon
07	modcal

The format of each file is as follows:

```
INTEGER LSTAT,ITYP
```

```
    INTEGER*2  JTB(6),JDATA(512),JNE,JTLMOD,JCLK
    read(5,5) JTB,JTLMOD,JNE,JCLK,ITYP,LSTAT
 5   format(10I5,Z10)
    read(6,6) (jdata(j),j=1,NCHN)o
 6   FORMAT(16i4)
```

where NCHN is 16 for JTLMOD = 3 and 4, 64 for JTLMOD=1, and 512 for JTLMOD=2. ITYP gives the type of calibrations (13, 10, 11, 07)

I have done some analysis and comparison of those files which I describe in

VoyMemo_198_V1_Mmode_modcals
VoyMemo_199_V1_Mmode_curcals
VoyMemo_210_V2_Mmode_modcals
VoyMemo_211_V2_Mmode_curcals
VoyMemo_212_V2_L_E1_E2_modcals

The two sections below give some information on *Modcals* and *Curcals.*

7.1.1 Modulator Voltage Calibration

The description below is from *VoyMemo_161_Modcal_Calibrations_Interpretation.pdf,* by Ralph L. McNutt Jr., dated 9/24/1987.

As part of the routine calibration sequence on the Voyager Plasma Science (PLS) experiment, there is a digitized readout of the low voltage signal which is proportional to the potential on the modulator grids. This is accomplished via a set of Modulator Voltage Monitors; these measurements are referred to by MVM on Summary or EDR tape logs. In many of the engineering notebooks they are referred to as "Modcal" measurements or mode (as compared to "Curcal" or current calibration measurements. In producing the modulator voltage, the voltage is stepped through one decade from 60 to 600 volts and then through the same steps with a extra gain of x 10 switched into the circuit to sweep from 600 to 6000 volts. To this voltage is added an offset of 50 volts. Hence, the L and M modes sweep from +10 V to +5950 V and the E2 mode sweeps from -10 V to -5950 V (the El mode sweeps from -10 V to 140 V by using a different step size). Thus, the true voltage ranges across 2.8 decades. The voltage monitors measure a voltage which is a constant fraction of the voltage swept which does not include the factor of 10 gain change. The monitors measure a voltage between 0.1 and 10 volts which is then input into a fast A/D converter. This voltage is then converted to a binary number from which the highest order bit is discarded. Thus, as the low voltage sweeps between 0.1 and 1.0 the digital output sweeps from 0 to 255; as the voltage sweeps from 1.0 to 10.0 volts, the output again sweeps from 0 to 255, although retention of the highest order bit would give a digital output from 256 to 511. Hence, the voltage monitor output can correspond to 4 orders of magnitude although, again, the factor of 10 gain change is not explicitly incorporated in this measurement. To know which decade is being read out, one must either rely on a "proper sequence" (the case for nominal operation for

which the MVM readout presumably yields voltages close to the nominal values) or an "educated guess" (for interpreting the MVM readouts from the PLS instrument on Voyager 1 after the failure).

Before the PLS instruments were to deliver to JPL for integration with the Voyager spacecraft, extensive calibration tests were run at the MIT Laboratory for Space Experiments using the Bench Checkout Equipment (BCE). The modulator was stepped through all channels in all modes and the DNS (or "decimal counts") were recorded as a function of step number, equal to the channel number minus one (channel 1 corresponds to step 0). In Appendix A, the reference counts are listed as a function of step number for each mode (labeled for the prototype rather than for one of the flight units). Corresponding voltages from the voltage monitors are also given. Note that these are the counts measured with the BCE. For example, the nominal value of VL for step 0 is +10 V in L and M modes and -10 V in El and E2 modes. The reference counts for the L, El, E2, and M modes are, respectively, 54, 48, 50, 48. The fraction values for VL are, presumably, the measured low voltage monitor outputs (they are not nominal values as the nominal value should be the same in for all of these). The applicable equation relating the monitor voltages and the reference counts is (4b). However, applying (4b) to values of 0.172, 0.163, 0.166, 0.163, yields DNS of 59.3, 53.3, 55.3, and 53.3, respectively. This suggests that the theoretical A/D algorithms are off (if the reference counts and monitor voltages were really measured simultaneously). Note that (4b) is off by about a factor of 105/256 = 1.046, but not quite. The agreement is better at the other end of the scale for vu of step 15 of E2 and L and step 127 of M, the counts are 248 and the monitor voltage is 9.314 V. Using 9.314 volts and equation (4a) yields a DN of 247.1. Again, if the counts and monitor voltages were measured at the same time (which is not known), there is some nonlinearity in the A/D converter, not currently accounted for. A spot check suggests that a simple DC offset voltage also does not account for the discrepancy.
To put all of this in perspective, at the higher voltages in the M mode, the reference counts for vu and VL are separated by 4 DN. This implies that a determination of the true potentials on the modulator grids to an accuracy of better than 1% should, in principal, be possible.

NOMINAL MONITOR OPERATION

In the usual MVM mode, the data numbers (DN) produced by running the low voltage monitor outputs through the fast A/D converter are returned as a function of channel number. In the L and M modes, the DNs corresponding to V_L are returned in the space occupied by A cup plasma measurements in the usual plasma measurement mode; similarly, the DNs corresponding to V_H are returned in the space occupied by the B cup plasma measurements. The C cup and D cup contain currents corresponding to normal plasma currents *but with DN values obtained from the fast A/D converter*. Hence, for the L and M modes, there is a measure of the contiguity of neighboring channels (gaps and/or overlaps in coverage).

For the E1 and E2 modes, there are only 16 slots available in the data sequence for each mode, so compromises were made in deciding which DN values would be included in the telemetry stream. For odd channel numbers (counting from 1 to 16), the DN corresponding to V_L is returned. For even channel numbers, the DN corresponding to V_U is telemetered. Hence, both absolute value and contiguity are checked, but only for every other channel. For example, there are MVM measurements for V_{L1}, V_{U2}, V_{L3}, V_{U4}, V_{L5}, etc., but there is no calibration information for the boundaries between channels 1 and 2, 3 and 4, etc.

In nominal operation, note that we should have $V_{U,\,n} = V_{L,\,n+1}$. Indication of where the V_Us and V_Ls come in the data is given in the VOYPRT appended to Voyager Memorandum 158 as Figure 6.

Attached as Appendix B are similar modulator calibration data from the Flight 1 unit (on Voyager 1, i.e., SN002). Most of the measurements are dated 4/22/77, less than 5 months before the launch. Unfortunately, simultaneous high voltage, monitor voltage, and DN were not recorded. It is worth noting that for step 127 of the M mode, the measured value of vu was 6010 volts, as compared to a nominal value of 5950 volts, a deviation from nominal of 1%. This suggests that such deviations are not uncommon.

7.1.2 Current Calibrations

NORMAL OPERATION

As part of the routine calibration sequence on the Voyager Plasma Science (PLS) experiment, there is a digitized readout of currents (DN or data numbers) produced by injected given currents into the measurement chain. This is done with the modulator on (modulator pickup calibration - AJ11) and with the modulator off (current calibration - AJ10). There are twelve different calibration currents which are injected into the measurement chain. These are labeled as I_0 through I_{11}. From 1/18/77 for Flight 1, the currents are as follows (all in amperes):

Current	Value
I_0	3.61×10^{-14}
I_1	1.64×10^{-13}
I_2	1.35×10^{-12}
I_3	1.81×10^{-12}
I_4	3.54×10^{-12}
I_5	1.61×10^{-11}
I_6	1.33×10^{-10}
I_7	1.77×10^{-10}
I_8	1.78×10^{-10}
I_9	8.07×10^{-10}
I_{10}	6.65×10^{-9}
I_{11}	8.88×10^{-9}

These are the same peak-to-peak calibration currents listed on p. IC-10 of the *Plasma Science Experiment Preliminary Design Review* of January 15, 1975.

In the E1 and M modes currents I_0 through I_{11} are injected starting in the channel 1 telemetry slot (in E1 currents I_0 through I_3 in channels 13 through 16; in M the 12 currents are injected cyclically 10 times - channels 1 through 120 and then I_0 through I_7 are injected in channels 121 through 128). The resulting data numbers are processed in the normal A/D mode. In the L and E2 modes currents I_0 through I_3 are injected in four cycles in channels 1 through 16; the measured currents are converted to DN using the *fast* A/D converter.

7.2 Daily and hourly averages, and fine resolution data

The process of making the hourly average files is described in *voyager_memos/pdf/VoyMemo_075_Voyager_Hourly_Average_Tapes.pdf,* see also *VoyMemo_119_Corrected_Hourly_Average_Tape_Format.pdf.*

The format of each type of file is given in a *AAA_readme.txt* file in each directory. Voyager 1 has no daily average file.

7.3 Mission Files (*vgr* files)

See the discussion of the history of the *Mission* files in Section 1.5.2 above, especially 1.5.2.3. Below is from the document *Voyager_PLS_v_02/documentation_v_02/general/vgr.pdf.*

To: Voyager Internal

From: G. S. Gordon Jr.

Subject: Voyager Mission Tape

Date: April 2, 1996

A compact summary of the entire Voyager mission is proposed below. The summary should contain all currents in all modes for some selection of the spectra. In addition it will contain the proton density, velocity and thermal width, as well as the B field for L and M modes. RTN coordinates will be used. Moment estimate will be used for the proton parameters, except for one thermal speed.

Tape Format

word	format	meaning	definition
1	I1	JTB(6)	time year, day, hour, min, sec, millisec/4, year = year-1900
			if day > 255 then day=day-256 ; hour=hour+100
			if tape was made on SUN and SC is Voyager 1 50 is added to hour
			if tape was made on SUN and SC is Voyager 2 25 is added to hour
	I1	MINDEX	first channel used (M mode only)
	I1	MODTLM	Telemetry mode from GSFC header
3	I1	LSTAT	Status word. zero if word is missing.
	I1	NCUR	Number of words of current. (number of current/4)
	I1	JTLMOD	Mode type. (1->L, 2->M, 3->E1, 4->E2)
	I1	JCLK	Cup integration time index. (1->30, 2->210, 3->930)
4	I1	JDATA	Digital currents. note only one byte per a measurement.
			for L & M modes
4+ncur	R4	DEN	ANS(38), Proton Density in number/cc
5+ncur	R4	VR	ANS(99), Proton Velocity in Km/sec
		VT	ANS(100)
		VN	ANS(101)
8+ncur	R4	Wm	(ANS(34)+ANS(35)+ANS(36))/3 Thermal width, moment.
9+ncur	R4	Wf	* Thermal width, fit.
10+ncur	R4	Dalpham	ANS(117), Alpha density in num/cc, moment.
11+ncur	R4	Dalphaf	ANS(59), Alpha density in num/cc, fit.
12+ncur	R4	BR	ANS(96), Magnetic Field in gamma
		BT	ANS(97)
		BN	ANS(98)
15+ncur	R4	R	Radial distance from sun in AU.

One spectra will be taken every 12 mins, for each mode, before Neptune. After Neptune every spectra is taken. For mission tapes generated at GSFC, the environmental variable SC must be set to identify

*

Wf = (Wa + Wb + Wc)/3
Wa = sqrt((WPER^2*(1-B.Na^2)) + (WPAR^2*(B.Na))^2)
WPER = ANS(69)
WPAR = ANS(68)
B.Na = ANS(130) (actually computed in program)

I have written a routine on *Solaris* that reads the original *binary* file and makes an *ascii* version. See *VoyMemo_214_converting_VGR_files_from_binary_to_ascii*. You can see the *Solaris* code that does this at */software_v_01/convert_vgr_binary_ascii.* The resultant *ascii* files are located in *Voyager_PLS_v_02/v1/vgr* and *Voyager_PLS_v_02/v2/vgr.*

7.4 Spectral Files and Color Spectrograms (*spc* files and plots)

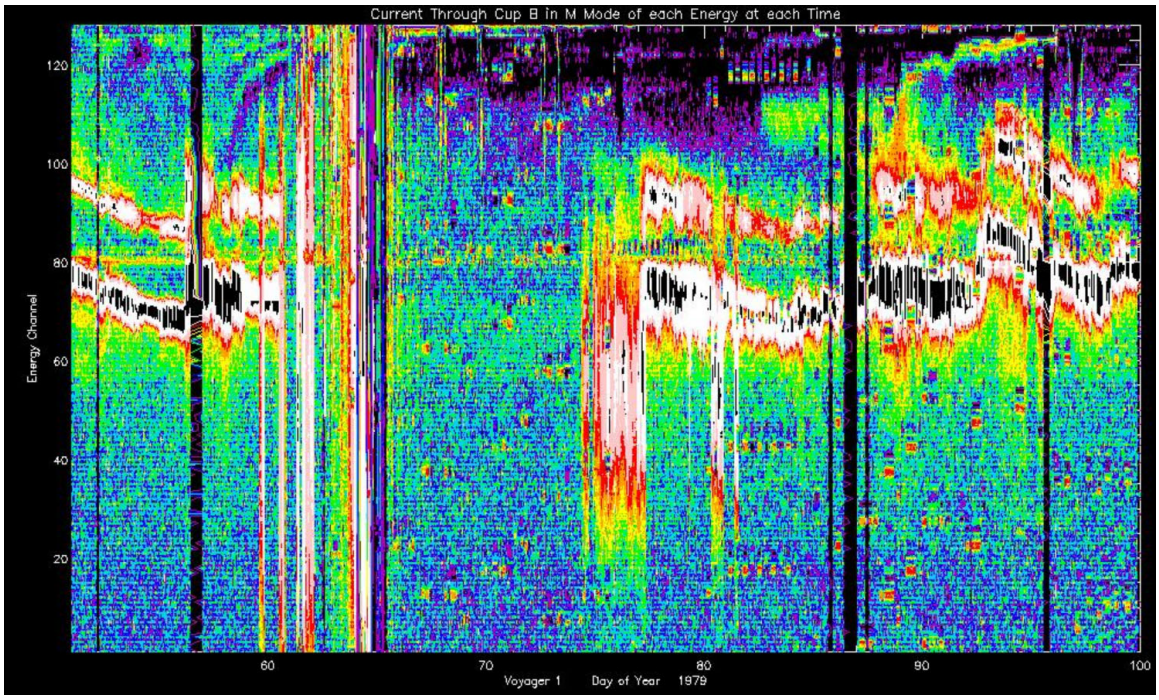

See Section 1.5.2.4 above. The *spc* files contain DN values for the currents, over the entire mission, and can be found at *Voyager_PLS_v_02/v1/spc/data* and *Voyager_PLS_v_02/v2/spc/data.* The corresponinging color spectograms for the data in each *spc* file can be found at *Voyager_PLS_v_02/v1/spc/plots* and *Voyager_PLS_v_02/v2/spc/plots.* There are 10 plots for each interval: the *A*, *B*, *C*, and *D*, cups in the *L* and *M* mode, and *E1* and *E2*. Above we show plots for *C* cup in the *M* mode for a period that includes the Voyager 1 Jupiter encounter. The color spectrograms for Voyager 1 are available up until the final failure. The color spectrograms for Voyager 2 go from launch to DOY 300 of 2020 (see *Voyager_PLS_v_02/v2/spc/plots/Acup_Mmode*). We ceased production of these spectrograms in 2020 because we were in the interstellar medium at that point and there was little information in them.

Leslie Finck produces new *V2all.txt* files as the data is put up at *JPL*, and then I turn them into the smaller *spc* files. My program to take a *v2all* file and make a *spc* file can be found at *software_v_01/spc_file_from_v12all_file*, see also Case 8 of *The Voyager PLS Utility Software.*

The color spectrograms are made in *idl* using an *idl* routine *SpectraPlotterTenPlots.* Although color spectrograms are useful, they usually contain many days, and this limits their usefulness. For example, below is the color spectrogram that shows *A cup M mode* measurements at the termination shock in 2007,

Voyager_PLS_v_02/v2/spc/plots/Acup_Mmode/v2_2007_201_250_Acup_Mmode.jpeg

This is part of a 50 day stretch of data.

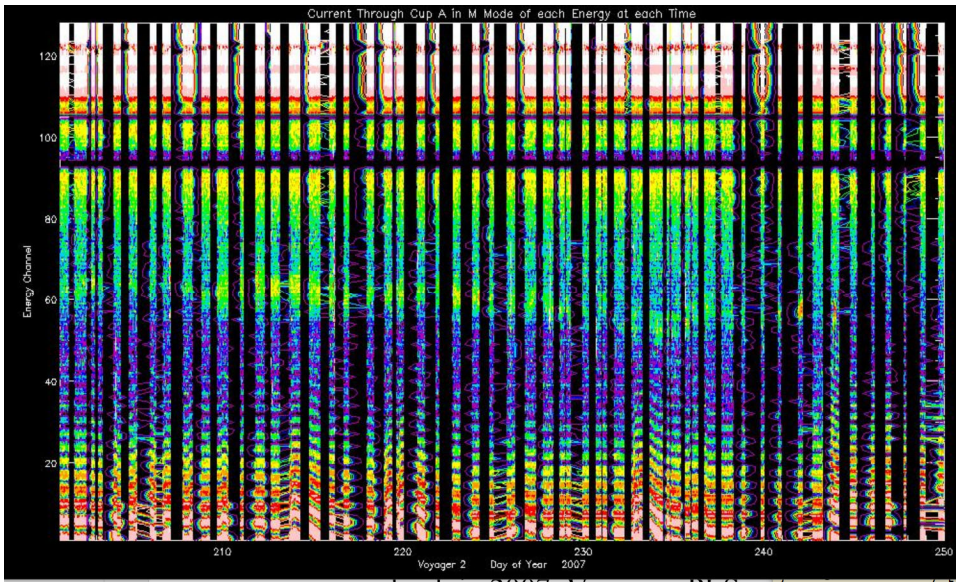

We show how to get the better resolution color spectrogram below on DOY 242 and 243 in 2007 in Case 9 of *The Voyager PLS Utility Software*, assuming the user has *idl* installed on their system. The plot below is the *A cup L mode* plot, which shows that we are in the solar wind at the beginning of DOY 242, cross the Termination Shock for the first time in a data gap, are in the heliosheath for most of DOY 243, and then return to the solar wind at the end of DOY 243.

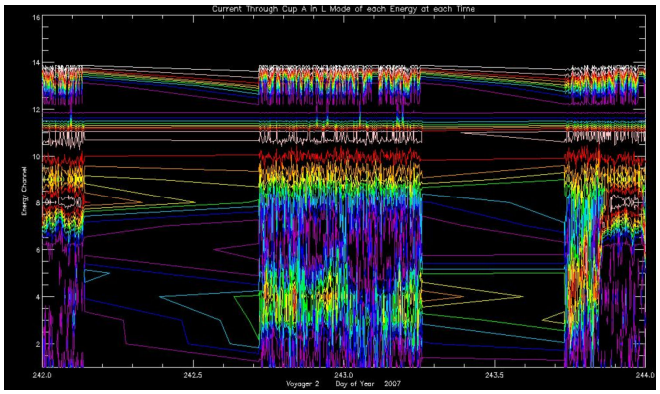

7.5 Encounter Files (*spl* files)

The encounter data for all encounters was written in the *spl* binary format. George Gordon Jr.'s memo on this is at *Voyager_PLS_v_02/documentation_v_02/general/spl.pdf*.

These have all been converted to *ascii* files, see:

for the format and the files that were included in our final files. Also reference the six Voyager Memos below:

VoyMemo_202_Neptune_Data
VoyMemo_203_Uranus_Data
VoyMemo_204_v2_Saturn_Data_v_02
VoyMemo_205_v2_Jupiter_Data_v_03
VoyMemo_206_v1_Jupiter_Data_v_02
VoyMemo_207_v1_Saturn_Data

In the new *ascii* versions, each measurment (L,E1,M,E2) mode has three files:

```
      INTEGER*2 JTB(6),JTLMOD,JCLK,MINDEX,KSTAT,IM,JDATA(512)
      INTEGER*2 JNE,LSTAT,IPLS,ITYP,KMOD,IDSC
      REAL CUR(512)
 1    READ(5,39,END=999) jtb,jtlmod,JNE,jclk,LSTAT,ITYP,MINDEX,
     * MODTAL,FACT,ICAP,IGAIN,IDSC
 39   FORMAT(9i5,Z6,2I5,I12,F10.2,3i3)
      READ(5,99) (JDATA(J), J = 1,JNE)
  99  FORMAT(16i4)
      READ(5,199) (CUR(J),J=1,JNE)
 199  FORMAT(8e12.4)
```

JTB(6): time
JTLMOD: mode
JNE: number of currents (16, 16, 64, and 512 for E1,E2,L,M)
JCLK: clock integration time
LSTAT: status word
ITYP: instrument state (plasma mod on is 15)
MINDEX: same as on original spl
MODTAL: same as on original spl
FACT: threshold current for this jclk, icap, and igain
ICAP: capacitor setting from lstat (0 or 1)
IGAIN: gain state from lstat (0 or 1)
IDSC: spacecraft (1 or 2)
JDATA: DN values
CUR: current in femtoamps if plasa mod on. If not, just DN values as real.

The other variables on the binary *spl* tapes I have not carried over to the new text versions.

7.6 Summary Files (*summary*)

The Voyager 1 PLS and MAG processing were done conjointly at *GSFC* in the initial phase of the mission (see Section 1.5.1 above).

The output of that processing was the *SUMMARY* tapes. The Voyager 1 *SUMMARY* tapes end on DOY 366 of 1980 and can be found in *Voyager_PLS_v_02/v1/summary.* The Voyager 2 *SUMMARY* tapes end on DOY 234 of 1989 and can be found in *Voyager_PLS_v_02/v2/summary_77_80, summary_81_84,* and *summary_85_89.*

I have written a read routine to read the plasma data on the summary tapes on *CentOS*, which can be found in *Voyager_PLS_v_02/software_v_01/summary_pls_read*. See Case 5, the *summary_pls_read* section, in the document *Voyager PLS Utility Software.*

I have attempted to write a read routine to read the magnetic field data on the *summary* tapes on *CentOS*, although I have not been successful in doing that. See *software_v_01/summary_mag_read* and Case 6 of *The Voyager PLS Utility Software.*

7.7 Experimental Data Record Files (*edr*)

These are the basic data records provided by JPL to *MIT*. See Voyager Memos 190, 191, and 192, and the document *Voyager_PLS_v_02/documentation_v_02/general/EDR_format_JPL.pdf* .

I include only those *edr* files that *MIT* received after the end of summary tape production at *GSFC* (beginning with *v2_edr_1990.260.10_1990.262.17*) up to the turn off on September 27, 2024.

I have written a read routine to read the *edr*'s on *CentOS*, even though they are generated on *Solaris*, which can be found in *Voyager_PLS_v_02/software_v_01/nxtedr_read*. See Case 11, the *nxtedr_read* section in the document *Voyager PLS Utility Software.*

8 Analysis of Data in the Interstellar Medium

8.1 Description

Voyager 2 crossed the heliopause in 2018, see *Richardson_Nature_2019_Heliopause.pdf.*

In the interstellar medium, the low temperatures imply that the instrument only measures significant data in the first channel of the *L* mode and in the lower channels of the *M* mode. Nonetheless we are still able to determine the properties of the Interstellar Medium by the roll modulation in those lower channel signals. The optimal roll orientation for detecting interstellar flow given the available lock stars was calculated in 1994, 24 years before the spacecraft crossed the heliopause (*VoyMemo_187_Optimal_Lock_Star_Heliosheath_Interstellar_Flow.pdf*).

The reason we can detect the interstellar medium even using only the lower channels is because that medium is transonic, so there is a strong asymmetry between looking into the flow and looking away from the flow, as is evident in the graph below.

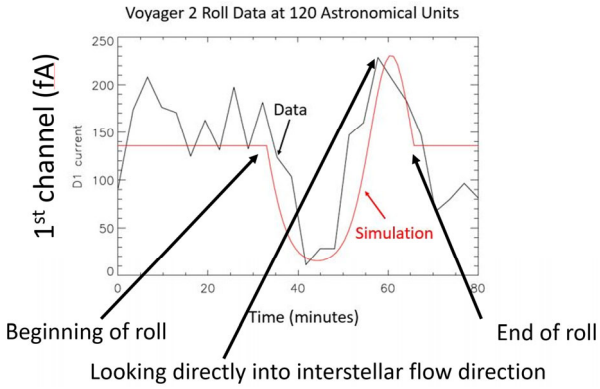

The "Simulation" shown in this figure was produced by the software program in the directory *software_v_01/ISM_roll_analysis*. We are able to estimate the density and temperaure of the Interstellar Mediium by varying input parameters to the simulation and determing the parameters that best fit the data.

The figure below shows our sensitivity to changes in temperature: hotter temperatures imply a more subsonic flow, and less variation through out the roll (very subsonic flows would show no variabion at all). Compare the 7500 K simulation curve below to the 8000 K simulation curve.

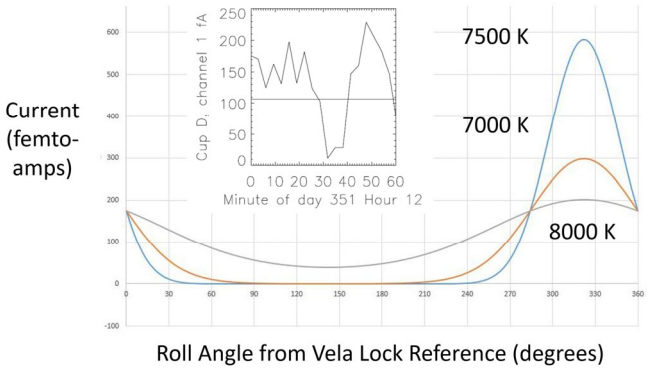

8.2 Roll Times

John Richardson has provided a complete list of the Voyager 2 roll times in the interstellar medium. In the first of these below, the sequence 351/12:33:24.442232 - SCE 18 is SCET (spacecraft event time) in 2018, followed by ERT (earth received time)

VOYAGER - 2 ONE REVOLUTION MAGROL
Add - 61 6 seconds (- 10 minutes - 1 6 seconds) of FDS clock drift to the SCE Times listed
Voyager - 2 2018 - 256 MAGROL version - 2 (Sequence B181) MAGROLS:
Two complete negative turn along the roll axis.
AC7TCD 321 033167 18 - 351/12:33:24.442232 - SCE 18 - 352/05:12:20.302 - ERT 04901:03:612F

CC7PC 345 18 - 351/13:08:34.493538 - SCE 18 - 352/05:47:30.527 - ERT 04901:47:580F
AC7TCD = 1 st Turn Starts
CC7PC 345 occurs approxim ately 2 minutes after the negative roll turn ends.
Each revolution takes approximately 33.3 minutes (2,000 seconds) .
SC21AF = CRS Command Words

VOYAGER - 2 ONE REVOLUTION MAGROL
Add - 628 seconds (- 10 minutes - 28 seconds) of FDS clock drift to the SCE Times listed
Voyager - 2 2019 - 023 MAGROL version - 1 (Sequence B182)
MAGROLS: One negative turn along the roll axis.
AC7TCD 321 033167 19 - 022/11:31:00.442227 - SCE 19 - 023/04:12:57.023 - ERT 05979:45:612F
CC7PC 345 19 - 022/12:06:10.493573 - SCE 19 - 023/04:48:07.144 - ERT 05980:29:580F
AC7TCD = 1 st Turn Starts
CC7PC 345 occurs approxim ately 2 minutes after the negative roll turn ends.
Each revolution takes approximately 33.3 minutes (2,000 seconds) .
SC21AF = CRS Command Words

V2_mags-2019ver2.pdf VOYAGER - 2 ONE REVOLUTION MAGROL
Add - 42.5 seconds (0 minutes - 42.5 seconds) of FDS clock drift to the SCE Times listed
Voyager - 2 2019 - 164 MAGROL version - 2 (Sequence B184)
MAGROLS: One negative turn along the roll axis.
AC7T CD 321 033167 19 - 164/23:31:00.442203 - SCE 19 - 165/16:10:47.811 - ERT 10254:45:612F
CC7PC 345 19 - 165/00:06:10.493576 - SCE 19 - 165/16:45:57.891 - ERT 10255:29:580F
AC7TCD = 1 st Turn Starts
CC7PC 345 occurs approxim ately 2 minutes after the negative roll turn ends.
Each revolution takes approximately 33.3 minutes (2,000 seconds) .

VOYAGER - 2 ONE REVOLUTION MAGROL
Add - 63 seconds (0 minutes - 03 seconds) of FDS clock drift to the SCE Times listed
Voyager - 2 2019 - 256 MAGROL version - 3 (Sequence B185)
MAGROLS: One negative turn along the roll axis.
AC7TCD 321 033167 19 - 255/17:31:00.442239 - SCE 19 - 256/10:20:02.069 - ERT 12977:15:612F
CC7PC 345 19 - 255/18:06:10.493576 - SCE 19 - 256/10:55:12.372 - ERT 12977:59:580F
AC7TCD = 1 st Turn Starts
CC7PC 345 occurs approxim ately 2 minutes after the negative roll turn ends.

Each revolution takes approximately 33.3 minutes (2,000 seconds).

VOYAGER 2 ONE REVOLUTION MAGROL (- 360 ❓)
Add - 1 70 seconds (- 2 minutes - 50 second s) of FDS clock drift to the SCE Times listed
Voyager - 2 202 0 - 0 25 MAGROL (Sequence B1 86)
MAGROL : One complete negative turn along the roll axis.
AC7TCD 321 033167 20 - 025/08:31:00.442206 - SCE 20 - 026/01:39:25.606 - ERT 17016:00:612F
CC7PC 345 20 - 025/09:06:10.493552 - SCE 20 - - 026/02:14:35.720 - ERT 17016:44:580F
AC7TCD = 1 st Turn Starts
CC7PC 345 occurs approxim ately 2 minutes after the negative roll turn ends .
Each revolution takes approximately 33.3 minutes (2,000 seconds)

VOYAGER 2 ONE REVOLUTION MAGROL (-360❓)
Add -183 seconds (-3 minutes -03 seconds) of FDS clock drift to the SCE Times listed
Voyager-2 2021-077 MAGROL (Sequence B191)
MAGROL: One complete negative turn along the roll axis.
AC7TCD 321 033167 21-077/05:31:00.442254-SCE 21-077/23:05:45.979-ERT 29552:15:612F
CC7PC 345 21-077/06:06:10.493551-SCE 21-077/23:40:55.982-ERT 29552:59:580F
AC7TCD = 1st Turn Starts
CC7PC 345 occurs approximately 2 minutes after the negative roll turn ends.
Each revolution takes approximately 33.3 minutes (2,000 seconds).

VOYAGER 2 ONE REVOLUTION MAGROL (-360❓)
Add -138 seconds (-2 minutes -18: seconds) of FDS clock drift to the SCE Times listed
Voyager-2 2021-168 MAGROL (Sequence B192)
MAGROL: One complete negative turn along the roll axis.
AC7TCD 321 033167 21-168/23:31:00.442246-SCE 21-169/17:03:42.604-ERT 32304:45:612F
CC7PC 345 21-169/00:06:10.493592-SCE 21-169/17:38:52.696-ERT 32305:29:580F
AC7TCD = 1 st Turn Starts i
CC7PC 345 occurs approximately 2 minutes after the negative roll turn ends.
Each revolution takes approximately 33.3 minutes (2,000 seconds).

VOYAGER 2 ONE REVOLUTION MAGROL (-360❓)
Add -222 seconds (-3 minutes -42 seconds) of FDS clock drift to the SCE Times listed
Voyager-2 2021-236 MAGROL (Sequence B193)
MAGROL: One complete negative turn along the roll axis.
AC7TCD 321 033167 21-235/18:31:00.442203-SCE 21-236/12:09:40.767-ERT 34308:30:612F
CC7PC 345 21-235/19:06:10.493527-SCE 21-236/12:44:51.034-ERT 34309:14:580F
AC7TCD = 1st Turn Starts

CC7PC 345 occurs approximately 2 minutes after the negative roll turn ends.
Each revolution takes approximately 33.3 minutes (2,000 seconds).

VOYAGER 2 ONE REVOLUTION MAGROL (-360°)
Add -222 seconds (-3 minutes -42 seconds) of FDS clock drift to the SCE Times listed
Voyager-2 2021-236 MAGROL (Sequence B193)
MAGROL: One complete negative turn along the roll axis.
AC7TCD 321 033167 21-235/18:31:00.442203-SCE 21-236/12:09:40.767-ERT 34308:30:612F
CC7PC 345 21-235/19:06:10.493527-SCE 21-236/12:44:51.034-ERT 34309:14:580F
AC7TCD = 1 st Turn Starts
CC7PC 345 occurs approximately 2 minutes after the negative roll turn ends.
Each revolution takes approximately 33.3 minutes (2,000 seconds).

VOYAGER 2 ONE REVOLUTION MAGROL (-360°)
Add -227 seconds (-3 minutes -47 seconds) of FDS clock drift to the SCE Times listed
Voyager-2 2021-259 MAGROL (Sequence B193)
MAGROL: One complete negative turn along the roll axis.
AC7TCD 321 033167 21-259/17:31:00.442255-SCE 21-260/11:13:34.328-ERT 35027:15:612F
CC7PC 345 21-259/18:06:10.493570-SCE 21-260/11:48:44.636-ERT 35027:59:580F
AC7TCD = 1 st Turn Starts i
CC7PC 345 occurs approximately 2 minutes after the negative roll turn ends.
Each revolution takes approximately 33.3 minutes (2,000 seconds).

VOYAGER 2 ONE REVOLUTION MAGROL (-360°)
Add -270 seconds (-4 minutes -50 seconds) of FDS clock drift to the SCE Times listed
Voyager-2 2022-077 MAGROL (Sequence B195)
MAGROL: One complete negative turn along the roll axis.
AC7TCD 321 033167 22-077/05:31:00.442244-SCE 22-077/23:32:08.617-ERT 40502:15:612F
CC7PC 345 22-077/06:06:10.493546-SCE 22-078/00:07:18.621-ERT 40502:59:580F
AC7TCD = 1 st Turn Starts
CC7PC 345 occurs approximately 2 minutes after the negative roll turn ends.
Each revolution takes approximately 33.3 minutes (2,000 seconds).

VOYAGER 2 ONE REVOLUTION MAGROL (-360°)
Add -316 seconds (-5 minutes) of FDS clock drift to the SCE Times listed
Voyager-2 2022-258 MAGROL (Sequence B197aa)
MAGROL: One complete negative turn along the roll axis.
AC7TCD 321 033167 22-257/17:31:00.442229-SCE 22-258/11:39:33.117-ERT 45917:15:612F
CC7PC 345 22-257/18:06:10.493544-SCE 22-258/12:14:43.421-ERT 45917:59:580F

AC7TCD = 1st Turn Starts
CC7PC 345 occurs approximately 2 minutes after the negative roll turn ends.
Each revolution takes approximately 33.3 minutes (2,000 seconds).

VOYAGER 2 ONE REVOLUTION MAGROL (-360°)
Add -430 seconds (-7 minutes -7 seconds) of FDS clock drift to the SCE Times listed
Voyager-2 2023-348 MAGROL (Sequence B202)
MAGROL: One complete negative turn along the roll axis.
AC7TCD 321 033167 23-348/10:31:00.475244-SCE 23-349/05:21:16.418-ERT
CC7PC 345 23-348/11:06:10.558431-SCE 23-349/05:56:26.685-ERT
AC7TCD = 1st Turn Starts
CC7PC 345 occurs approximately 2 minutes after the negative roll turn ends.
Each revolution takes approximately 33.3 minutes (2,000 seconds).

VOYAGER 2 ONE REVOLUTION MAGROL (-360°)
Add -455 seconds (-7 minutes -35 seconds) of FDS clock drift to the SCE Times listed
Voyager-2 2024-072 MAGROL (Sequence B203)
MAGROL: One complete negative turn along the roll axis.
AC7TCD 321 033167 24-072/04:31:00.471284-SCE 24-072/23:25:02.493-ERT
62251:00:613F
CC7PC 345 24-072/05:06:10.552348-SCE 24-073/00:00:12.534-ERT
62251:44:581F
AC7TCD = 1st Turn Starts
CC7PC 345 occurs approximately 2 minutes after the negative roll turn ends.
Each revolution takes approximately 33.3 minutes (2,000 seconds).

VOYAGER 2 ONE REVOLUTION MAGROL (-360°)
Add -479 seconds (-7 minutes -59 seconds) of FDS clock drift to the SCE Times listed
Voyager-2 2024-165 MAGROL (Sequence B203)
MAGROL: One complete negative turn along the roll axis.
AC7TCD 321 033167 24-165/22:31:00.474408-SCE 24-166/17:22:47.840-ERT
65063:30:613F
CC7PC 345 24-165/23:06:10.558147-SCE 24-166/17:57:57.955-ERT
65064:14:581F
AC7TCD = 1st Turn Starts
CC7PC 345 occurs approximately 2 minutes after the negative roll turn ends.
Each revolution takes approximately 33.3 minutes (2,000 seconds).

Voyager 2 2024-257 MAGROL (Sequence: B205)
VOYAGER 2 ONE REVOLUTION MAGROL (-360°)
Add -503 seconds (-8 minutes -23 seconds) of FDS clock drift to the SCE Times listed
AC7TCD 321 033167 24-256/16:31:00.472530-SCE 24-257/11:32:02.161-ERT
62251:00:613F
CC7PC 345 24-256/17:06:10.554480-SCE 24-257/12:07:12.493-ERT
62251:44:581F

AC7TCD = 1st Turn Starts CC7PC 345 occurs approximately 2 minutes after the negative roll turn ends.
Each revolution takes approximately 33.3 minutes (2,000 seconds).

9 Data from the Last EDR

The PLS experiment was turned off on September 27, 2024.

Below is data from the final edr, *pls24271.b*. I give the last E1, L, E2 , M before turn off and the first after turn off.

The last M mode of the E1, L, E2 , M sequence is at 2024 271 7 53 8 677.

E1 MODE
2024 271 7 52 5 325 3 16 3 111 1 3 6F6F0000
0 0 99 123 99 0 0 47 123 104 94 0 35 97 127 78

L MODE
2024 271 7 52 26 437 1 16 3 47 1 3 2F2F0000
0 99 123 0 127 92 0 127 70 58 145 145 162 182 195 200
0 89 0 0 85 0 0 71 0 0 52 33 0 0 91 0
0 112 0 0 93 0 105 59 0 122 92 96 132 133 134 128
0 31 118 65 0 0 0 114 94 87 120 128 146 157 177 192

E2 MODE
2024 271 7 52 47 565 4 16 3 175 1 3 AFAF0000
122 128 114 0 0 105 122 122 63 0 32 122 113 0 0 223

M MODE
2024 271 7 53 8 677 2 128 3 239 1 3 EFEF0000
79 108 122 0 139 73 86 127 0 121 110 0 133 71 0 119
0 0 110 0 68 108 0 0 93 0 97 99 0 66 98 0
64 97 0 82 84 0 20 97 0 31 87 0 0 72 0 0
67 0 255 255 0 0 0 0 0 0 0 0 0 0 0 0
0 0 0 0 0 0 0 0 0 0 0 0 0 0 0 0
0 0 0 0 0 0 0 0 0 0 0 0 0 0 0 0
0 0 0 0 0 0 0 0 0 0 0 0 0 0 0 0
0 0 0 0 0 0 0 0 0 0 0 0 0 0 0 0
0 82 75 0 73 0 69 60 0 86 0 29 86 0 43 68
0 72 57 0 60 56 0 78 0 51 60 0 0 42 80 0
0 59 0 0 64 0 0 0 0 43 0 0 57 23 65 62
12 0 255 255 0 0 0 0 0 0 0 0 0 0 0 0
0 0 0 0 0 0 0 0 0 0 0 0 0 0 0 0
0 0 0 0 0 0 0 0 0 0 0 0 0 0 0 0
0 0 0 0 0 0 0 0 0 0 0 0 0 0 0 0

0 0 0 0 0 0 0 0 0 0 0 0 0 0 0 0
0 116 0 98 78 0 109 0 53 94 0 101 0 0 93 0
0 97 0 0 95 0 0 79 0 0 93 0 39 70 0 0
0 0 20 47 0 0 0 57 0 52 0 62 63 0 0 0
9 0 255 255 0 0 0 0 0 0 0 0 0 0 0 0
0 0 0 0 0 0 0 0 0 0 0 0 0 0 0 0
0 0 0 0 0 0 0 0 0 0 0 0 0 0 0 0
0 0 0 0 0 0 0 0 0 0 0 0 0 0 0 0
0 0 0 0 0 0 0 0 0 0 0 0 0 0 0 0
128 90 86 0 81 109 67 81 0 85 99 68 55 0 0 104
81 0 90 0 23 102 0 85 0 0 0 90 0 10 88 0
65 91 0 0 99 54 47 67 0 0 84 69 0 68 0 33
79 68 255 255 0 0 0 0 0 0 0 0 0 0 0 0
0 0 0 0 0 0 0 0 0 0 0 0 0 0 0 0
0 0 0 0 0 0 0 0 0 0 0 0 0 0 0 0
0 0 0 0 0 0 0 0 0 0 0 0 0 0 0 0
0 0 0 0 0 0 0 0 0 0 0 0 0 0 0 0

E1 MODE
2024 271 7 55 17 323 3 16 3 0 0 0 0
0 0 0 0 0 0 0 0 0 0 0 0 0 0 0 0

L MODE
2024 271 7 55 38 436 1 16 3 0 0 0 0
0 0 0 0 0 0 0 0 0 0 0 0 0 0 0 0
0 0 0 0 0 0 0 0 0 0 0 0 0 0 0 0
0 0 0 0 0 0 0 0 0 0 0 0 0 0 0 0
0 0 0 0 0 0 0 0 0 0 0 0 0 0 0 0

E2 MODE
2024 271 7 55 59 564 4 16 3 0 0 0 0
0 0 0 0 0 0 0 0 0 0 0 0 0 0 0 0

M MODE
2024 271 7 56 20 676 2 128 3 0 0 0 0
0 0 0 0 0 0 0 0 0 0 0 0 0 0 0 0
0 0 0 0 0 0 0 0 0 0 0 0 0 0 0 0
0 0 0 0 0 0 0 0 0 0 0 0 0 0 0 0
0 0 0 0 0 0 0 0 0 0 0 0 0 0 0 0
0 0 0 0 0 0 0 0 0 0 0 0 0 0 0 0
0 0 0 0 0 0 0 0 0 0 0 0 0 0 0 0
0 0 0 0 0 0 0 0 0 0 0 0 0 0 0 0
0 0 0 0 0 0 0 0 0 0 0 0 0 0 0 0
0 0 0 0 0 0 0 0 0 0 0 0 0 0 0 0
0 0 0 0 0 0 0 0 0 0 0 0 0 0 0 0

0 0 0 0 0 0 0 0 0 0 0 0 0 0 0 0
0 0 0 0 0 0 0 0 0 0 0 0 0 0 0 0
0 0 0 0 0 0 0 0 0 0 0 0 0 0 0 0
0 0 0 0 0 0 0 0 0 0 0 0 0 0 0 0
0 0 0 0 0 0 0 0 0 0 0 0 0 0 0 0
0 0 0 0 0 0 0 0 0 0 0 0 0 0 0 0
0 0 0 0 0 0 0 0 0 0 0 0 0 0 0 0
0 0 0 0 0 0 0 0 0 0 0 0 0 0 0 0
0 0 0 0 0 0 0 0 0 0 0 0 0 0 0 0
0 0 0 0 0 0 0 0 0 0 0 0 0 0 0 0
0 0 0 0 0 0 0 0 0 0 0 0 0 0 0 0
0 0 0 0 0 0 0 0 0 0 0 0 0 0 0 0
0 0 0 0 0 0 0 0 0 0 0 0 0 0 0 0
0 0 0 0 0 0 0 0 0 0 0 0 0 0 0 0
0 0 0 0 0 0 0 0 0 0 0 0 0 0 0 0
0 0 0 0 0 0 0 0 0 0 0 0 0 0 0 0
0 0 0 0 0 0 0 0 0 0 0 0 0 0 0 0
0 0 0 0 0 0 0 0 0 0 0 0 0 0 0 0
0 0 0 0 0 0 0 0 0 0 0 0 0 0 0 0
0 0 0 0 0 0 0 0 0 0 0 0 0 0 0 0
0 0 0 0 0 0 0 0 0 0 0 0 0 0 0 0
0 0 0 0 0 0 0 0 0 0 0 0 0 0 0 0

10 List of Voyager Memos

I have gone through the entire set of the historic memos and only included those memos I judged to be important. Note that word versions of the more recent Voyager Memos (*VoyMemo_190_Processing_EDR_File.doc* through *VoyMemo_217_timing_problems_2023_107.doc*) are in *Voyager_PLS_v_02/documentation_v_02/voyager_memos/word_docs.*

VoyMemo_001_FTS_Line_June_02_1977.pdf
VoyMemo_021_PLS_Program_Package.pdf
VoyMemo_028_Calibration_CR-1.pdf
VoyMemo_033_Rotate_from_SC_Coordinates.pdf
VoyMemo_042_Jovian_Encounter_Timelines.pdf
VoyMemo_044_SEDR_Predict_Eath_Jupiter.pdf
VoyMemo_046_Trip_Report_GSFC.pdf
VoyMemo_048_Time_Solar_Wind_Move_2pts.pdf
VoyMemo_049_Interpolation_SEDR_data.pdf
VoyMemo_050_Trip_Report_GSFC.pdf
VoyMemo_051_Trip_Report_GSFC.pdf
VoyMemo_052_Eliminating_Spikes_Proton_Spectra.pdf
VoyMemo_055_Trip_Report_GDFC.pdf
VoyMemo_056_In_House_Data_Processing.pdf
VoyMemo_075_Voyager_Hourly_Average_Tapes.pdf
VoyMemo_078_LECP_Stepping_V2_Saturn_Encounter.pdf
VoyMemo_079_GSFC_1800_Encounter_Plots.pdf
VoyMemo_080_Uranus_Encounter_Sampling_Scheme.pdf

VoyMemo_081_Meetings_and_Deadlines.pdf
VoyMemo_083_Optimal_Orientation_Uranus_Ring_Plane.pdf
VoyMemo_086_LELE_Plasma_Sample_Uranus.pdf
VoyMemo_087_Plasma_At_Uranus_Ring_Plane.pdf
VoyMemo_088_Current_Status_Voyager_2.pdf
VoyMemo_092_Types_of_Voyager_Data_Received_at_CSR.pdf
VoyMemo_095_Magnetospheric_Data_Analysis.pdf
VoyMemo_096_Comparison_of_ABSOM_and_ABSO.pdf
VoyMemo_097_JPL_Uranus_Neptune_SWG_April_12_1984.pdf
VoyMemo_099_Comparison_VGRANAL_and_MJSANL.pdf
VoyMemo_100_Comparison_Fits_Bagenal_McNutt_MJSANL.pdf
VoyMemo_101_JPL_Uranus_Neptune_SWG_May_21_1984.pdf
VoyMemo_103_Comparison_Single_Double_Precision_Barnet_routines.pdf
VoyMemo_104_Comparison_Spectral_Fits_McNutt_MJSANL.pdf
VoyMemo_106_Uranus_SSG_Nov_20_1984.pdf
VoyMemo_109_Uranus_SSG_March_18_1985.pdf
VoyMemo_111_SC_Attitude_Uranus_Near_Encounter.pdf
VoyMemo_112_Storage_MJSANL_Fits.pdf
VoyMemo_114_Problems_L_Short_New_Uranus_Format.pdf
VoyMemo_115_Magnetospheric_Data_Analysis.pdf
VoyMemo_116_SSG_June_24_1985.pdf
VoyMemo_118_Limitations_on_Bimaxwellian_Simulation_Code.pdf
VoyMemo_119_Corrected_Hourly_Average_Tape_Format.pdf
VoyMemo_122_GSFC_Spectral_Plots_Uranus_Encounter.pdf
VoyMemo_123_Read_Routines_Extended_Cruise_Uranus_Encounter.pdf
VoyMemo_124_Voyager_2_SEDR_Data_Sets.pdf
VoyMemo_125_Data_GSFC_for_MJSANL.pdf
VoyMemo_126_GSFC_PreUranus_Visit_Dec_17_1985.pdf
VoyMemo_128_Decrease_LABBI_Runtime.pdf
VoyMemo_129_V2_Uranus_VMV_Plots_DOY_24.pdf
VoyMemo_133_Read_Voyager_Data_Fits.pdf
VoyMemo_134_Gaps_V2_Uranus_Encounter_Data_Set.pdf
VoyMemo_135_Calculating_Plasma_Densities_Io_Torus.pdf
VoyMemo_136_Comparison_Ion_Electron_Densities_Jup_Sat_Uranus.pdf
VoyMemo_138_Implementation_MJSANL_on_SUN.pdf
VoyMemo_139_Timing_Olberts_New_Simulation.pdf
VoyMemo_140_Data_Files_Fits_Spectra_Jovian_Magnetosphere.pdf
VoyMemo_141_LECP_Stepping_and_PLS_Data_Uranus.pdf
VoyMemo_141_LECP_Stepping_PLS_Data_Uranus.pdf
VoyMemo_142_SSG_Meeting_Nov_17_1986.pdf
VoyMemo_143_Reading_Mag_Data_from_Summary_File.pdf
VoyMemo_144_Roll_Orientation_Neptune_and_VIM_inputs.pdf
VoyMemo_145_Implementation_MJSANL_on_SUNS.pdf
VoyMemo_146_SWG_Meetings_2_23_87_SSG_3_5_87.pdf
VoyMemo_147_Bug_in_MJSANL_on_SUNS.pdf
VoyMemo_148_Use_Of_Input_File_with_MJSANL.pdf
VoyMemo_149_LECP_Stepping_at_Neptune.pdf
VoyMemo_152_Loss_of_Data_Mode_Changes_Uranus.pdf
VoyMemo_153_Failure_V1_Post_Saturn.pdf
VoyMemo_154_Failure_V1_Post_Saturn_More.pdf
VoyMemo_155_Failure_V1_Temp_Variations.pdf
VoyMemo_156_Photoelectrons_In_Side_Sensor.pdf
VoyMemo_157_Failure_V1_DC_Return_Currents.pdf
VoyMemo_158_Failure_V1_Temperature_Extremes.pdf

VoyMemo_160_Post_Neptune_Cruise_5_and_7.pdf
VoyMemo_161_Modcal_Calibrations_Interpretation.pdf
VoyMemo_162_Calibration_V1_Post_Failure.pdf
VoyMemo_165_Distribution_Fns_PLS_LECP.pdf
VoyMemo_168_Short_Encounter_SEDR_with_REVISION.pdf
VoyMemo_169_commands.pdf
VoyMemo_170_calibrations_in_VIM.pdf
VoyMemo_173_Error_in_SXRED_Program.pdf
VoyMemo_174_changes_in_cruise_processing.pdf
VoyMemo_174_In_House_Processing_V2_Data.pdf
VoyMemo_176_Changes_in_Cruise_Data_Processing.pdf
VoyMemo_176_cruise_processing.pdf
VoyMemo_178_Gain_States_Calibration_Neptune_Encounter.pdf
VoyMemo_180_Trajectory_Files_Cruise_3_Revisions.pdf
VoyMemo_182_Overview_VIM-5.pdf
VoyMemo_183_DC_Return_Calibration_Data_V1_V2.pdf
VoyMemo_184_Extracting_Engineering_Data_EDRs.pdf
VoyMemo_187_Optimal_Lock_Star_Heliosheath_Interstellar_Flow.pdf
VoyMemo_188_Neptune_Trajectory_Parameters.pdf
VoyMemo_189_Voyager_DSN_Tracking_Reduction.pdf

VoyMemo_190_Processing_EDR_File.pdf
VoyMemo_191_Format_Records_EDR.pdf
VoyMemo_192_New_Version_nxtedr_v_02.pdf
VoyMemo_193_Converting_Encounter_SPL_Files_to_Text_files.pdf
VoyMemo_194_Archiving_Cruise_Spectral_Data.pdf
VoyMemo_195_Running_mjsanl_Carrington.pdf
VoyMemo_196_Checking_New_JPL_EDR_v_02.pdf
VoyMemo_197_calibration_files.pdf
VoyMemo_198_V1_Mmode_modcals.pdf
VoyMemo_199_V1_Mmode_curcals.pdf
VoyMemo_200_Planetary_SSEDR_Files_v_02.pdf
VoyMemo_201_MJSANAL.pdf
VoyMemo_202_Neptune_Data.pdf
VoyMemo_203_Uranus_Data.pdf
VoyMemo_204_v2_Saturn_Data_v_02.pdf
VoyMemo_205_v2_Jupiter_Data_v_03.pdf
VoyMemo_206_v1_Jupiter_Data_v_02.pdf
VoyMemo_207_v1_Saturn_Data.pdf
VoyMemo_208_Encounter_SEDR.pdf
VoyMemo_209_EDR_Problems.pdf
VoyMemo_210_V2_Mmode_modcals.pdf
VoyMemo_211_V2_Mmode_curcals.pdf
VoyMemo_212_V2_L_E1_E2_modcals.pdf
VoyMemo_213_converting_Cruise_SHORTSEDR_from_binary_to_ascii.pdf
VoyMemo_214_converting_VGR_files_from_binary_to_ascii.pdf
VoyMemo_215_Processing_EDRs__to_v2all_files_on_Faraday_v_02.pdf
VoyMemo_216_Porting_MJSANL_to_CentOS_and_Fedora.pdf
VoyMemo_217_timing_problems_2023_107.pdf

11 Differences between VOY_PLS_V01 and VOY_PLS_V02

Important note: on the original *VOY_PLS_V01* flash drive I had not properly untarred the spectrogram plots from Voyager 1 onto the flash drive itself (they were properly in the tar files on *VOY_PLS_V01* and if you untarred them using *script_for_PLS_deploy* you got everything correctly installed on the laptop you were transferring them to)

But the *script_for_PLS_deploy_flashdrive* on *VOY_PLS_V01* had an error in it such that the Voyager 1 histogram plots were not included the flash drive itself in *E:\Voyager_PLS_v_01\v1\spc*). If you have one of these flash drives *VOY_PLS_V01* **please rename and repurpose it**, so that copies of this are not floating around. The *script_for_PLS_deploy_flashdrive* on *VOY_PLS_V02* has been corrected.

The contents of *Voyager_PLS_v_01/documentation_v_01* has been changed in *Voyager_PLS_v_02/documentation_v_02.* The ***only*** change is in *Voyager_PLS_v_02/documentation_v_02/general,* where we have replaced the document *VoyagerInterstellar_v_06.doc* with *VoyagerInterstellar_v_07.doc* (this document) and *VoyagerInterstellar_v_06.pdf* with *VoyagerInterstellar_v_07.pdf.*

The directory *Voyager_PLS_v_02/software_v_01* is ***identical*** to *Voyager_PLS_v_01/software_v_01.*

The file *Voyager_PLS_v_02.tar.gz* is identical to *Voyager_PLS_v_01.tar.gz.*

The files *VOY_PLS_V02_readme.txt*, *script_for_PLS_deploy*, and *script_for_PLS_deploy_flashdrive* have been changed appropriately to refer to the appropriate files for *VOY_PLS_V02.*

I have added a list of the roll times for Voyager 2 in the interstellar medium in Section 8.2 above.

I have added some data from the last edr for Voyager 2 in Section 9 above.

All the data files for Voyager 2 on *VOY_PLS_02* are identical to those on *VOY_PLS_01* except for the following:

In *VOY_PLS_01,* the directory *Voyager_PLS_v_01/v2/edr/2023* only went up to *V2_edr_2023.229.10_2023.236.02.gz*. On *VOY_PLS_02,* it now finishes out the year and there is a new directory *Voyager_PLS_v_02/v2/edr/2024* with 2024 data up until *V2_edr_2024.272.05_2024.272.09.gz*. This last file is from after the turn-off and has no data. The file *V2_edr_2024.271.06_2024.271.22.gz* has the last data; the last M mode of the E1, L, E2 , M sequence is at 2024 271 7 53 8 677. See Section 9 above.

In *VOY_PLS_01,* the directory *Voyager_PLS_v_01/v2/spc/data* only went up to *v2_spc_2023.229.10_2023.236.02.txt.gz*. The data in *Voyager_PLS_v_02/v2/spc/data* continues until *v2_spc_2024.271.06_2024.271.22.txt.gz*.